UNIVERSIDADE D
COIMBRA

Inês Ralha Correia Bem-Haja

RESPONSE TO INTRANASAL OXYTOCIN DURING EMOTION RECOGNITION IN SCHIZOPHRENIA: A PHARMACO-NEUROIMAGING STUDY

Dissertação no âmbito do Mestrado em Engenharia Biomédica orientada pela Doutora Diana Maria Pinto Prata, pelo Professor Doutor Miguel de Sá e Sousa de Castelo-Branco e pelo Doutor Philippe Pinel e apresentada ao Departamento de Física da Faculdade de Ciências e Tecnologias.

Setembro de 2023

Response to Intranasal Oxytocin during Emotion Recognition in Schizophrenia: a Pharmaco-Neuroimaging Study

Inês Ralha Correia Bem-Haja

A thesis submitted for the degree of Master in Biomedical Engineering

Supervisors:
Doutora Diana Maria Pinto Prata
Prof. Doutor Miguel de Sá e Sousa de Castelo-Branco
Doutor Philippe Pinel

Department of Physics
University of Coimbra
Portugal

September 2023

Agradecimentos

Este trabalho nunca teria sido possível sem o apoio e orientação de tantas pessoas. Em primeiro lugar, gostaria de expressar o meu mais profundo agradecimento aos meus supervisores, Diana Prata, Professor Miguel Castelo-Branco e Philippe Pinel. Eles ajudaram-me a superar os meus desafios através da sua compreensão e do tempo dedicado. Foi uma honra e um privilégio estar rodeado de investigadores com um vasto conhecimento neste campo, a neurociência.

Estendo estes últimos sentimentos a todos os investigadores do Laboratório da Diana Prata. Obrigado pelo vosso compromisso com a ciência, bem como pelas questões que colocaram nas minhas apresentações. Aos alunos de doutoramento, Vasco Sá e Gonçalo Cosme, por tirarem algum tempo da vossa atarefada agenda para me ajudar quando estava perdida. Além disso, estou especialmente grata à Rute Patuleia, que percorreu esta jornada comigo enquanto nos apoiávamos mutuamente na nossa tese.

Quando iniciei a minha carreira nas ciências, tive de enfrentar o meu desconforto em relação à matemática. Na escola, sempre tive dificuldades, e foi com a ajuda da minha explicadora de matemática, Dra. Olga, que comecei a sentir-me mais à vontade e confiante. As palavras não podem expressar o impacto que ela teve na minha vida, por isso, a ela, estendo um agradecimento inimaginável.

Aos meus amigos, obrigado. Obrigado por serem os meus apoiantes. Sempre que me sentia insegura ou incapaz, vocês estavam sempre lá para me trazer de volta à realidade.

Por último, mas não menos importante, à minha base, a minha família. Vocês moldaram quem sou e despertaram o meu interesse pela neurociência. Sem vocês, eu não estaria aqui hoje. Serei eternamente grata a vocês.

Acknowledgements

This work would never have been possible without the support and guidance of so many people. First and foremost, I would like to show my deepest level of gratitude to my supervisors, Diana Prata, Professor Miguel Castelo-Branco, and Philippe Pinel. They have helped me overcome my struggles through their understanding and the time they have devoted. It was an honour and a privilege to be surrounded by researchers with such a vast knowledge of this field, neuroscience.

Furthermore, I extend these last sentiments to all the researchers at Diana Prata's Lab. Thank you for your commitment to science as well as the questions you posed in my presentations. To the seniors, Vasco Sá and Gonçalo Cosme, for taking some time out of your busy PhD schedule to help me when I was lost. Furthermore, I am especially grateful towards Rute Patuleia, who rode this wave with me as we supported each other through our thesis research.

When I embarked on my career in the sciences, I had to confront my uneasiness with mathematics. At school, I struggled, and it was with the help of my math tutor, Dr. Olga, that I began to feel more comfortable and confident. Words cannot express the impact she had on my life, therefore, to her, I extend an unimaginable thank you.

To my friends, thank you. Thank you for being my cheerleader. Whenever I felt unsure or incapable, you were always there to snap me back to reality.

Last but not least, to my foundation, my family. You made me who I am and sparked my interest in neuroscience. Without you, I would not be here today. I will forever be grateful to you.

Resumo

A esquizofrenia é uma forma de transtorno mental que exerce um impacto substancial no funcionamento social. Uma das questões predominantes é a dificuldade em reconhecer emoções faciais, o que está intimamente relacionado com a necessidade frequentemente identificada de tratamento para abordar a função social inadequada. Estudos recentes sugerem que a oxitocina pode melhorar a perceção social em indivíduos com esquizofrenia, oferecendo uma possível via para intervenção terapêutica. No entanto, os resultados desses estudos têm sido inconclusivos, deixando incerteza sobre quais aspectos da cognição social podem ser melhorados pela oxitocina e como esta deve ser utilizada terapeuticamente. Este estudo teve como objetivo avaliar o efeito de uma única administração intranasal de oxitocina na atividade cerebral em indivíduos com esquizofrenia, utilizando um paradigma de reconhecimento de emoções faciais. Trinta e cinco utentes elegíveis do sexo masculino, que receberam oxitocina (24 UI) ou placebo, e vinte e um indivíduos saudáveis do sexo masculino participaram num estudo de sessão única, pseudo-randomizado, em dupla ocultação e controlado por placebo no Hospital Júlio de Matos do Centro Hospitalar Psiquiátrico de Lisboa. Foi realizada uma análise de região de interesse das respostas da amígdala esquerda ao teste de reconhecimento de emoções para comparar as condições dos medicamentos. Não foram encontradas evidências que sugerissem que a oxitocina teve um efeito maior na cognição social do que o placebo. Contrariamente a outros estudos, não foram observadas diferenças estatisticamente significativas na atividade da amígdala em resposta a rostos felizes e assustados quando induzidos pelo spray intranasal. Não foram detetados efeitos distintos da oxitocina entre os grupos de pacientes e controlo. Além disso, a oxitocina intranasal não reduziu a atividade da amígdala em resposta a rostos emocionais em pacientes com esquizofrenia, nem levou a um aumento significativo da atividade da amígdala em controlos saudáveis. Estes resultados destacam a necessidade imperativa de novas pesquisas destinadas a elucidar se a oxitocina possui o potencial para abordar défices na cognição social e/ou mitigar sintomas negativos em indivíduos com esquizofrenia.

Palavras-chave: Esquizofrenia, Oxitocina, fMRI, SPM, Reconhecimento de emoções.

Abstract

Schizophrenia is a form of mental disorder that exerts a substantial impact on social functioning. One of the predominant issues is the difficulty in recognising facial emotions, which is closely linked to the frequently identified need for treatment aimed at addressing inadequate social functioning. Recent studies suggest that oxytocin may enhance social perception in individuals with schizophrenia, offering a potential avenue for therapeutic intervention. Nevertheless, the outcomes of these studies have yielded inconclusive results, leaving uncertainty about which aspects of social cognition may be improved by oxytocin and how it should be used therapeutically. This study aimed to assess the effect of a single intranasal administration of oxytocin on brain activity in patients with schizophrenia, using a facial emotion recognition paradigm. Thirty-five eligible male patients were administered either oxytocin (24 IU) or placebo, and twenty-one healthy male control subjects participated in a single-session, pseudo-randomised, double-blind, placebo-controlled study at the Hospital Júlio de Matos of Centro Hospitalar Psiquiátrico de Lisboa. A region of interest analysis of the responses of the left amygdala to the emotion recognition test was conducted to compare drug conditions. No evidence was found to suggest that oxytocin had a greater effect on social cognition than the placebo. Contrary to other studies, no statistically significant differences in amygdala activity were observed in response to happy and fearful faces when induced by the intranasal spray. No distinctive effects of oxytocin were detected between the patient and control groups. Furthermore, intranasal oxytocin did not reduce amygdala activity in response to emotional faces among patients with schizophrenia, nor did it lead to a significant increase in amygdala activity in healthy controls. These findings underscore the imperative necessity for further research endeavours aimed at elucidating whether oxytocin holds the potential for addressing deficits in social cognition and/or mitigating negative symptoms in individuals with schizophrenia.

Keywords: Schizophrenia, Oxytocin, fMRI, SPM, Emotion recognition.

Contents

List of Figures

List of Tables

List of Abbreviations

3D Three-dimensional

AAL3 Automated Anatomical Labelling 3

AC Amygdaloid Complex

ANCOVA Analysis of Covariance

ANOVA Analysis of Variance

AVP Arginine Vasopressin

BNST Bed Nucleus of the Stria Terminalis

BOLD Blood Oxygenation Level-Dependent

CBF Cerebral Blood Flow

CeA Central Nucleus of the Amygdala

CHPL Centro Hospitalar Psiquiátrico de Lisboa

CSF Cerebrospinal Fluid

CTL Controls

dbRCT Double-Blind Randomised Controlled Trial

Df Degrees of Freedom

DSM Diagnostic and Statistical Manual of Mental Disorders

DRD2 Dopamine D2 Receptor

EPI Echo-Planar Imaging

FA Flip Angle

FD Framewise Displacement

FGA First Generation Antipsychotic

fMRI Functional Magnetic Resonance Imaging

FOV Field of View

FWHM Full-Width Half-Maximum

GLM General Linear Model

GM Grey Matter

GP Glycopeptide

GPCR G Protein-Coupled Receptor

GRE Gradient-Recall Echo

GRF Gaussian Random Field Theory

HRF Hemodynamic Response Function

IBEB Institute of Biophysics and Biomedical Engineering

ICD International Classification of Diseases

IGR Intergenic Region

IN-OT Intranasal Oxytocin

INU Intensity Non-Uniformity

LTI Linear and Time Invariant

MRI Magnetic Resonance Imaging

NMDA N-Methyl-D-Aspartate

NP Neurophysin

NPS Non Polydipsic

OT Neuropeptide Oxytocin

PBO Placebo

PCP Phenylcyclohexyl Piperidine

PPI Prepulse Inhibition

PS Polydipsic

PVN Paraventricular Nuclei

RF Radiofrequency

ROI Region-of-Interest

SCZ Schizophrenia

SD Standard Deviation

SGA Second Generation Antipsychotic

SNR Signal-to-Noise Ratio

SON Supraoptic Nuclei

SP Signal Peptide

SPM Statistical Parametric Mapping

T1w T1-weighted

TE Echo Time

ToM Theory of Mind

TR Repetition Time

WM White Matter

Chapter 1

Introduction

1.1 Contextualisation

Social cognition, although defined in many ways, generally refers to a neurocognitive operation that underlies social interaction [8]. This intricate mechanism enables individuals to make sense of various social cues, such as facial expressions, body language, and verbal communication, and to deduce the emotions, intentions, and mental states of those surrounding them [6]. Specifically, it pertains to how individuals perceive, process, and interpret social information, encompassing a range of higher- and lower-order skills [9]. For example, the Theory of Mind (ToM), or mental state attribution, is a cognitive ability in which mental states, such as thoughts, beliefs, desires, and intentions, are assigned to oneself and others, to explain, manipulate, and predict behaviour. Lower-order skills are automatic processes involving fast cue detection and judgement, such as eye-gaze and emotional recognition [10]. The amygdala emerges as a pivotal central neural region implicated in orchestrating these intricate processes [11]. Disruptions in these mechanisms manifest in a spectrum of neuropsychiatric disorders, including but not limited to autism, bipolar disorder, and schizophrenia (SCZ) [12].

SCZ is marked by both positive and negative symptoms, as well as cognitive impairments [9]. The use of antipsychotics has led to a decrease in the intensity of positive symptoms, such as paranoid delusions and auditory hallucinations [6]. However, there has not been a significant reduction in the severity of negative symptoms, which include withdrawal from interpersonal relationships and anhedonia [6]. These negative symptoms are believed to be an external manifestation of social cognitive deficits [6]. Consequently, to improve the quality of life of patients with SCZ, it is essential to comprehend the mechanisms underlying these relationships.

Various hypotheses have been proposed to explain SCZ's neuropathophysiology, including the dopamine and serotonin hypotheses. However, research has shown that oxytocin (OT) is a promising molecule [6]. OT is a neuropeptide hormone that acts as a neuromodulator [13]. It is released in response to positive social interactions such as physical touch, eye contact, and nurturing behaviours, and its primary purpose is to promote social bonding and attachment [2]. Recent studies have focussed on the deregulation of the oxytocinergic system in schizophrenia [14].

The primary imaging method favoured by researchers is functional magnetic resonance imaging (fMRI). This technique provides valuable insights into brain connectivity by measuring variances in blood flow that correspond to neuronal activity [15, 16]. Real-time acquisition of images from participant groups is followed by image processing to remove physiological artefacts, allowing comparisons between different groups [15]. Together with statistical parametric mapping

(SPM), researchers are able to analyse brain activation in various regions and make inferences about specific effects of interest.

1.2 Objectives and Hypotheses

This dissertation aims to investigate the relationship between OT and SZC during the emotional recognition paradigm. For this purpose, three groups were included: SZC patients who had taken intranasally administered OT (SZC-OT), SZC patients who took placebo (SZC-PBO), and healthy controls.

We hypothesise that patients administered OT have amygdalar activation in the emotion recognition task more similar to healthy controls than patients who had taken the placebo (PBO). Furthermore, we also consider whether OT concentration levels modulate the activation of specific brain areas in SZC and control subjects.

1.3 Document Structure

This thesis is organised as follows: Chapter 2 touches on the theoretical background necessary for the development of the work; Chapter 3 reviews the literature; Chapter 4 gives us a detailed description of the methodology, including population description, methods and fMRI preprocessing data; Chapter 5 presents the results while also discussing them, and Chapter 6 concludes the dissertation with the main conclusions and possible future developments.

Chapter 2

Background Knowledge

Within the confines of this chapter, a thorough and all-encompassing examination is conducted regarding the fundamental principles that hold the utmost relevance to this dissertation. Through this meticulous exploration, a more detailed and heightened clarification of the concepts introduced in the previous Chapter 1 is realised.

2.1 Exploring the Dynamics of Social Cognition: A Comprehensive Analysis

Social cognition is a fundamental part of human psychology, allowing us to comprehend, interpret, and interact with the social world [6]. It is a multifaceted cognitive domain that encompasses empathy, ToM, emotion recognition, and attribution, all of which are essential for the development of meaningful relationships [9].

Social skills start to form as early as 14 months of age and are necessary throughout life. To create appropriate social interactions, various distinct processes must be employed. These include the identification of others through facial expressions, gestures, postures, body language, and voice. This information is then used to create a direct resonance of others' emotional states (empathy) and to interpret their observable behaviours (ToM). This lays the groundwork for three fundamental domains of social cognition: social perception, social understanding, and social decision-making. These processes are impaired in a number of pathologies, such as neuropsychiatric disorders (e.g. SCZ), leading the DSM-5 (Diagnostic and Statistical Manual of Mental Disorders, 5th Edition) to recognise social cognition as an essential factor for the social engagement of many individuals [12].

2.1.1 The Face Emotion Recognition Paradigm: Mechanisms and Applications

Facial expressions are of great importance as visual signals for humans, and their associated emotions significantly shape our perceptions, decisions, and interactions [17]. The capacity to recognise and understand emotions, both in ourselves and others, is a key factor in successful communication and meaningful social interactions. In this context, the task of face emotion recognition is a multidisciplinary paradigm that evaluates social cognition by assessing an individual's ability to identify emotions expressed through static images or dynamic facial expressions [18]. Professor Paul Ekman's compilation known as *"Ekman's Faces"*, includes the representation

of six basic emotions: disgust, anger, fear, surprise, sadness, and happiness. These emotions, which all humans can identify and express regardless of their sociocultural background [12], are designed to provide varying levels of difficulty and to cover the range of potential deficits. They are presented in a range of intensities and in a variety of experimental settings [19]. However, the available evidence on the interaction between cultural norms and facial expression processing, as well as the interpretation of emotions, supports the "interactionist perspective", which takes into account the combined influence of biological and cultural factors [12].

Research efforts applying face emotion recognition techniques are characterised by a certain degree of heterogeneity due to various methodological factors. However, these studies suggest that the ability to detect socially relevant information does not depend on localised neural regions. Instead, it relies on a complex neural network that processes social cues and connects this knowledge to areas of the brain responsible for motivation, emotion, and adaptive behaviours [19]. These regions, including the amygdala, prefrontal cortex, and insula, work together to interpret facial expressions, vocal tones, body language, and contextual clues to identify emotional states.

2.2 The Amygdala: Unravelling the Key Enigma of Emotional Processing

Nestled deep in the temporal lobe of the brain, the amygdala has emerged as a critical hub for processing emotions, memories, and responses to environmental stimuli [20]. Its intricate role in shaping human behaviour and the complex interplay between cognitive and affective processes has made it a focal point of study in neuroscience.

The amygdala, composed of almond-shaped clusters containing 13 nuclei collectively known as the Amygdaloid Complex (AC), is situated bilaterally and symmetrically within the medial temporal lobes. These nuclei are categorised into three groups: deep or basolateral, cortical-like, and superficial or centromedial, shown in Figure 2.1. Additionally, the various nuclei within the AC are intricately interconnected with various brain regions, encompassing the prefrontal cortex, hippocampus, and sensory processing areas. This extensive connectivity facilitates the amygdala in orchestrating a wide range of emotional and cognitive responses based on sensory input and past experiences [21].

As mentioned above, at the core of its functioning, the amygdala's role is in processing emotions, particularly fear and threat detection. Incoming sensory information from the environment is rapidly relayed to the amygdala, which then assesses the emotional significance of the stimulus. In instances of potential danger, the amygdala triggers the "fight-or-flight" response, mobilising the body to respond appropriately to threats [22]. Furthermore, the amygdala also plays a role in social-emotional processing. It aids in interpreting facial expressions and other non-verbal cues, contributing to the perception of emotions in oneself and others. In particular, the recognition of primary facial expressions transcends cultural boundaries and is uniformly recognised across diverse cultures around the world. However, nuanced assessment of the intensity of these expressions depends on the cultural context [23].

Deficits in amygdala function can impair social interactions and emotional comprehension, as observed in conditions such as SCZ. Studies have demonstrated that individuals with SCZ often exhibit altered amygdala activity and connectivity, which may contribute to difficulties in recognising emotions and navigating social situations [24]. Understanding the intricate role of the amygdala and its implications for conditions like SCZ provides valuable insights into the underlying mechanisms of social cognition and emotional processing.

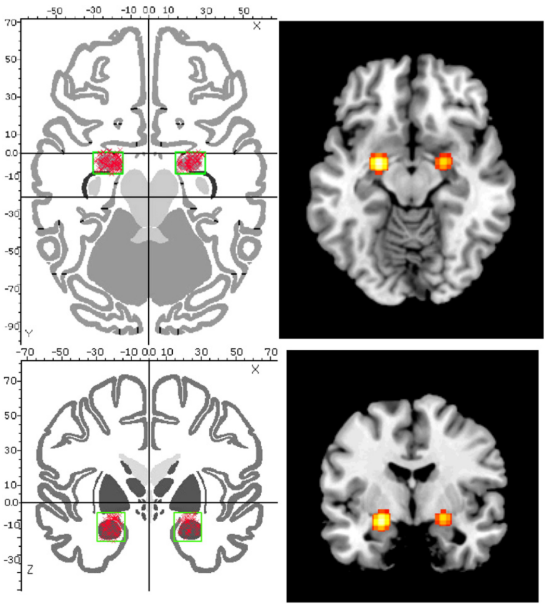

Figure 2.1: Localisation of amygdala activation foci and regions exhibiting statistically significant activation density is depicted in axial (z = -12) and coronal (y = -4) slices within the Talairach space. Each activation focus is symbolised by a red. The green boxes mark the Region-of-Interest (ROI), outlining the outermost coordinates of amygdala tissue as defined in the Talairach and Tournoux Atlas. The accompanying images on the right showcase regions with a statistically significant density of activation peak occurrences. *Adapted from [1].*

2.3 Schizophrenia: Dissecting the Complexities of a Multifaceted Disorder

Schizophrenia is a perplexing mental disorder affecting around 1% of the world's population. It places a significant weight on the patient, due to the high costs of hospitalisation and medical care, as well as psychological impairments such as depression, cognitive deficits, and social dysfunction. This collective burden further contributes to their disproportionate presence in homeless communities [25].

The DSM-5 is used by mental health professionals to diagnose, classify, and recognise various mental health conditions. According to the DSM-5, schizophrenia is diagnosed when the patient exhibits two or more of the five unique symptoms linked to psychotic disorders, such as delusions, hallucinations, or disorganised thinking, shown in Table 2.1. These symptoms must be active for at least one month and the overall duration of the disease must be at least six months [26].

Even though brain development abnormalities associated with schizophrenia may begin during the prenatal period, it is not commonly observed in childhood, with an incidence rate lower than 0.04% [27]. Generally, schizophrenia tends to emerge during late adolescence or early adulthood, with slightly later onset in women [28].

The prevailing pharmacological approach to treating schizophrenia is antipsychotic medications. These medications can be divided into two categories [29]: typical or first-generation antipsychotics (FGAs), and atypical or second-generation antipsychotics (SGAs). Both categories of medications inhibit the functioning of the dopamine D2 receptor (DRD2), resulting in a reduction in positive symptoms. Even though there are no significant differences in efficacy between the two categories, FGAs are more related with extrapyramidal side effects, namely dystonic reactions and Parkinsonian symptoms. On the other hand, SGAs correspond to a

heightened risk of inducing weight gain and metabolic disruptions. This difference in adverse effects may be explained by the fact that FGA tends to linger longer on DRD2, whereas SGA acts on other receptors, including the serotonin 2A receptor [5]. As mentioned in Chapter 1 Section 1.1, there has been no significant reduction in the severity of negative symptoms by any class of antipsychotics [6].

Symptom Cluster	**Clinical Examples**
Positive Symptoms	Delusions Hallucinations Disorganised speech
Negative Symptoms	Avolition Anhedonia Alogia
Affective Symptoms	Depression Anxiety Affective flattening
Cognitive Symptoms	Attention Memory Executive function

Table 2.1: Symptom Clusters and Clinical Examples in Schizophrenia. *Adapted from [5].*

2.3.1 Deciphering Social Cognition Impairments in Schizophrenia

Research has indicated that individuals with SCZ have a deficit in social cognition, which includes difficulty recognising expressions, emotions, and intentions. This can have a negative impact on their social, professional, and personal lives [30]. Therefore, these components of social cognition are essential to consider when providing psychosocial rehabilitation for people with SCZ [31].

It has been observed that although most patients understand the general aspects of social interactions, those with low functioning, who have more severe impairments in social cognition, have different levels of functioning, symptoms, and non-social cognition compared to those with high functioning [30].

Most of the research on SCZ has focused on ToM, emotional processing, and attributional biases. On the contrary, investigations of social perception and knowledge have been limited and have used different methods. People with SCZ have been found to have reduced performance in contextual fluency, interpretation, and following social conventions, but this is not necessarily correlated with the severity of their symptoms [31].

When using facial affect perception tasks and single-person video scenarios with various facial expressions, vocal intonations, and body gestures, it was found that those classified as high-functioning still had social perception abilities, while those considered low-functioning did not [32]. Another study showed that people with SCZ can use available contextual cues to understand ambiguous facial expressions [33].

2.4 Oxytocin: The Peptide Hormone's Physiological and Psychological Significance

The term "Oxytocin" originated from Greek words meaning "quick birth", following the observation of its uterine-contracting properties [34]. Since then, OT has been described as the "bonding hormone" due to its involvement in social behaviour, reproductive function, and even psychological states [2].

OT is a hydrophilic cyclic hormonal neuropeptide, composed of nine amino acids with a sequence of Cys–Tyr–Ile–Gln–Asn–Cys–Pro–Leu–GlyNH_2 (illustrated in Figure 2.2) [6]. It has a sulphur bridge between the two cysteines, which is similar to the arrangement of another nonapeptide, vasopressin (AVP). The OT gene is located on the same chromosome as AVP - chromosome 20 - yet its transcriptional direction is opposite in humans. Both are characterised by three exons and two introns, exhibiting a notable degree of similarity. Separating these two genes is an intergenic region (IGR). Currently, OT is known to have only one receptor (OTR) that falls within the rhodopsin-type (class I) G protein-coupled receptor (GPCR) family, and its coupling with phospholipase C occurs through $G_{\alpha q11}$ [14, 35].

Synthesised primarily in the hypothalamus and subsequently released by the posterior pituitary gland into the bloodstream, where it engages with its receptors in both the peripheral and central nervous systems, OT is subject to precise regulation by a variety of factors. It is predominantly produced within magnocellular neurosecretory neurones located in the paraventricular (PVN) and supraoptic (SON) nuclei. After synthesis, oxytocin is transported and stored in axon-terminal Herring bodies before being discharged into circulation via the neurohypophysis. This orchestration leads to peripheral effects, such as parturition and lactation [6]. Moreover, OT's influence extends to dendrites, where it governs its own release and maintains control over neuron firing patterns. In addition to its central role, smaller parvocellular neurons in the PVN and specific brain structures like the bed nucleus of the stria terminalis (BNST), medial preoptic area, and lateral amygdala contribute to localised release within the brain [2].

Numerous studies have established a link between OT levels and behaviour [36]. This hormone has the ability to enhance social recognition and reduce autonomic and endocrine stress, thus facilitating prosocial behaviour. While OT is associated with various "non-social" behaviours, including learning, anxiety, feeding, and pain perception, its roles in diverse social behaviours have garnered recent attention. OT plays a crucial role in social memory and attachment, sexual and maternal conduct, as well as aggression. Recent research has also implicated OT in human bonding and trust. Furthermore, OT expression could potentially be involved in human disorders characterised by atypical social interactions, such as autism and SCZ [2].

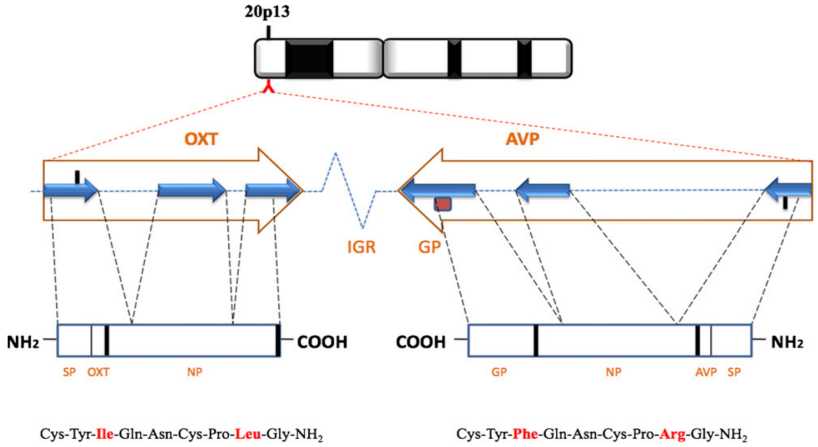

Figure 2.2: Diagram illustrating the gene structures of OT and AVP (indicated by prominent arrows), their corresponding preprohormones (enclosed in boxes), and the resultant neuropeptides (depicted at the bottom). Human chromosomal positions are displayed in the upper section. Both genes comprise three exons, denoted by small blue arrows, and are interspersed by two introns (represented as dashed lines connecting the exons). Despite residing on the same chromosome, these genes exhibit opposing transcriptional orientations and are demarcated by an intergenic region (IGR). The length of this IGR varies among species. Within the preprohormones, each component includes a signal peptide (SP), a neuropeptide (AVP or OT), and a neurophysin (NP), with the addition of a glycopeptide (GP) in the case of AVP. Protein processing signals are depicted as bold lines. Cysteine residues interact to form a disulfide bond, resulting in a cyclic six-amino acid ring structure in both neuropeptides. Notably, seven out of the nine amino acids remain consistent in the neuropeptides, while two differ (highlighted in red). *Adapted from [2].*

2.4.1 Oxytocin in Schizophrenia Behaviours

Over the years, research into the relationship between SCZ and OT has grown, providing insight into their connection. Both preclinical and clinical studies have suggested that oxytocin is involved in SCZ [14]. It has been observed that adult males with paranoid SCZ have higher cerebrospinal fluid (CSF) OT levels, and patients with SCZ, particularly those taking neuroleptics, have increased plasma OT levels [37]; however, not all studies agree [38]. Recently, it has been proposed that higher plasma OT levels in patients with SCZ may be due to a compensatory response to reduced sensitivity of OTRs to circulating hormone levels [14].

Individuals with SCZ often exhibit deficits in sensorimotor gating, such as the phenomenon of prepulse inhibition (PPI) of the startle reflex. This process involves the reduction of the reflexive response to a robust sensory stimulus due to the presence of a weaker sensory stimulus that precedes it. This gating mechanism serves as an attentional filter, allowing the individual to focus on pertinent information [2]. Studies have shown that OT can improve PPI disruption caused by drugs such as dizocilpine (a non-competitive N-methyl-D-aspartate (NMDA) antagonist) and amphetamine (an indirect dopamine agonist) [39].

Beyond its PPI effects, chronic administration of phenylcyclohexyl piperidine (PCP) produces social deficits and reduces OT binding in the hypothalamus. Conversely, it increases OT binding in the central nucleus of the amygdala (CeA). Interestingly, bilateral OT administration to CeA effectively reverses the social deficits arising from PCP. Furthermore, among individuals with SCZ, plasma OT levels are positively correlated with their ability to discern facial emotions, further linking OT with the social aspects of SCZ [2].

OT has demonstrated the potential to enhance social perception among individuals with SCZ [40]. Nevertheless, there remains an ongoing investigation into the precise impact of OT on

the neural activity underlying facial emotion recognition in the context of SCZ. This research promises to shed further light on the intricate interplay between OT and the cognitive and social deficits observed in this disorder, potentially opening avenues for novel therapeutic approaches.

2.5 Functional Magnetic Resonance Imaging: A Window into Brain Function

Functional Magnetic Resonance Imaging (fMRI) stands as a pivotal tool in modern neuroimaging, offering an unparalleled view into the functioning of the human brain [15]. This non-invasive technique has revolutionised the field of cognitive neuroscience by allowing researchers to visualise and comprehend brain activity during various tasks, emotions, and states of consciousness [41]. This is achieved primarily by leveraging the blood oxygenation level-dependent (BOLD) contrast mechanism, which effectively detects the increased local oxygenation that accompanies neural actions. These oxygenation shifts stem from fluctuations in blood flow and volume [16,42]. fMRI boasts remarkable spatial resolution, albeit at the cost of temporal resolution, while excelling in its ability to reveal subtle soft tissue distinctions [41]. This proficiency offers invaluable insights into the neural networks that underlie intricate cognitive processes.

2.5.1 Foundations of Magnetic Resonance Imaging

fMRI is a specialised form of Magnetic Resonance Imaging (MRI) that focusses on the particular regions of the brain responsible for controlling essential functions. Its fundamentals are based on the wider MRI technology [43]. MRI is an imaging technique that produces a map of the hydrogen nuclei (^{1}H) in different tissues [43]. These nuclei, mainly found in water and lipids in the body, have a property known as nuclear spin angular momentum. When exposed to a strong and unchanging magnetic field (B_0), these nuclear spins divide into two distinct energy levels: a lower state (parallel alignment to B_0) and a higher state (antiparallel alignment to B_0), changing their energy state and eventually creating a map [43]. Notably, an excess of protons accumulates in the lower energy state. These spins then rotate around the B_0 direction (also described as precess), with a frequency of rotation (Larmor frequency) proportional to the strength of B_0 [43]:

$$\omega_0 = \gamma B_0 \tag{2.1}$$

Here, γ is the gyromagnetic ratio, which remains constant for certain nuclei. Protons have the ability to both absorb and emit radiofrequency (RF) energy, a process activated by the application of an external magnetic field (B_1) orientated perpendicular to the static field B_0. These energy absorption and emission leads the protons to transition to higher or lower energy states, respectively. The total magnetic moments of all protons, referred to as net magnetisation, cause fluctuations in voltage within a wire coil [41]. This received signal, named the "free induction decay," oscillates at frequency ω_0 and decreases with time due to transverse relaxation [44].

The particles reside in a three-dimensional (3D) space distribution around B_0 (longitudinally), where precession also occurs. Upon the application of the RF pulse, the net magnetisation shifts to the transverse direction. Following the cessation of the RF pulse, the nuclei revert to an equilibrium ratio through longitudinal regrowth and transverse relaxation. The energy decay

manifests itself in two forms: *spin-lattice decay* (characterised by the time constant T_1) and *spin-spin decay* (marked by the time constant T_2). The values of these time constants vary depending on the types of particles and the characteristics of the surrounding material [45]. For example, the values vary based on tissue properties, enabling tissue differentiation.

Transverse relaxation is practically characterised by T_2^* values, which take into account differences in the magnetic field throughout the human body, leading to a faster decrease in signal. These discrepancies come from the non-uniformity of the magnetic field created by the magnet over the body and are affected by the distinct magnetic susceptibilities of various tissues. Changes in T_2^* have an effect on the magnetic resonance signal and are especially useful for recognising changes in brain hemodynamics caused by neuronal activity [41].

2.5.2 Fundamental Principles of BOLD Signal Dynamics

fMRI is typically obtained using the Blood Oxygenation Level-Dependent (BOLD) contrast mechanism, which provides an indirect measure of neuronal activity [42]. This technique relies on the different magnetic susceptibilities of haemoglobin, depending on whether it is oxygenated (Hb) or deoxygenated (dHb); Hb is a diamagnetic molecule, whereas dHb has paramagnetic properties [46].

In regions where the number of Hb molecules exceeds the number of dHb molecules, the magnetic resonance (MR) signal will increase. This phenomenon is due to the diamagnetic nature of the molecules, which causes them to repel magnetic fields, while paramagnetic molecules exhibit an attraction to the magnetic field. Thus, upon activation of brain regions, there is a simultaneous increase in metabolic demand, cerebral blood flow (CBF), and volume. As blood flow provides an oxygen surplus beyond the requirements for neuronal activity replenishment, a localised rise in Hb concentration occurs in contrast to the surrounding tissue, leading to an augmentation of the MR signal [47]. This phenomenon is elucidated by the correlation between elevated blood oxygenation (resulting in decreased dHb levels) and subsequent increase in T_2 and T_2^*, which ultimately results in a subtle signal enhancement in T_2 and T_2^*-weighted images [48, 49].

2.5.3 The Hemodynamic Response Function: Neural Activity's Blood Flow Signature

The hemodynamic response function (HRF) represents the temporal trajectory of the BOLD response ensuing the instigation of neuronal activity. Two vital aspects of the HRF demand attention when conducting an fMRI analysis.

In contrast to neuronal activity, the hemodynamic response is slow-paced, with neuronal activity typically lasting a few milliseconds, whereas the hemodynamic response lasts 12-18 seconds. The BOLD response may commence with a negative dip, manifesting approximately 1 to 2 seconds following the stimulus. This dip is related to oxygen consumption prior to any shifts in CBF and blood volume [50]. Subsequently, a peak emerges around 4 to 6 seconds after stimulation, with its magnitude reflecting the extent of neuronal activity within the tissue [16]. Following this peak, a post-stimulus undershoot could occur, spanning up to 20 seconds post-stimulus and culminating in a return to baseline.

Furthermore, the connection between the BOLD response and neuronal activity adheres to the characteristics of a linear and time-invariant (LTI) system [43]. This signifies that should a neural response undergo a scaling factor of a, the BOLD response will undergo an equivalent scaling by the same factor a [43]. Similarly, if the neural response experiences a delay of b

seconds, the BOLD response will exhibit a corresponding delay of b seconds. This feature facilitates the prediction of the BOLD response following a specific neural reaction through the convolution of the stimulus time series with an HRF [43]. In the context of fMRI analysis, the canonical HRF is commonly employed, namely the double gamma HRF. This HRF is rooted in the linear combination of two gamma functions, as illustrated in Figure 2.3 [51]. Its mathematical formulation is expressed as:

$$h(t) = A\left(\frac{(t^{\alpha_1})^{-1}\cdot\beta_1^{\alpha_1}\cdot e^{-\beta_1 t}}{\Gamma(\alpha_1)} - c\frac{(t^{\alpha_2})^{-1}\cdot\beta_2^{\alpha_2}\cdot e^{-\beta_2 t}}{\Gamma\Gamma(\alpha_2)}\right) \tag{2.2}$$

where

$$\Gamma(n) = (n-1)!(n>0) \tag{2.3}$$

α_1, α_2, β_1, β_2, and c are pre-established, whereas A represents the undisclosed amplitude and $\Gamma(n)$ signifies the gamma function [3]. The initial peak is influenced by the first gamma function, whereas the post-stimulus undershoot is modulated by the second.

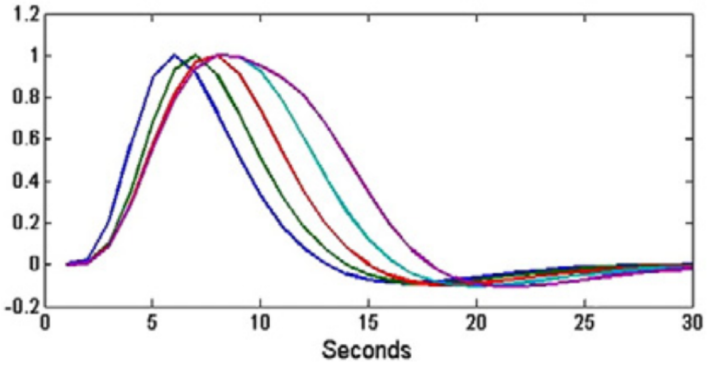

Figure 2.3: The canonical HRF is convolved with five stimulus functions of varying durations (ω), resulting in the illustration above. This visual representation highlights differences in time-to-peak and width, which are influenced by changes in duration. *Adapted from [3].*

2.5.4 Statistical Parametric Mapping: Revealing Patterns in Neuroimaging Data

Statistical Parametric Mapping (SPM) is a popular analytical technique for functional imaging studies, particularly those related to regional brain activation [52]. It involves the development of spatially extended statistical procedures to test hypotheses about localised effects in certain areas [53]. An SPM is an image composed of voxels that are similar to 3D pixels [52]. These voxel values are distributed based on a known probability density function under a null hypothesis, usually using the Student's T or F tests. They are also informally referred to as T- or F-maps. The success of SPM relies on the individual analysis of each voxel using a conventional statistical test, which is used to determine if a given voxel's time-series shows a systematic association with an explanatory variable. The parameters estimated individually are then combined into an image known as a statistical map [54].

Statistical Parametric Mapping (SPM) combines the General Linear Model (GLM) and Gaussian Random Field (GRF) theory to analyse and draw conclusions from continuous data. The GLM is used in identifying the parameters that explain the data, while RFT is employed

to address the issue of multiple comparisons when all voxel data are combined into a statistical map. This is done by adjusting the p-values for the search volume [54].

2.5.4.1 Delving into Analysis: The General Linear Model Perspective

Examining imaging data requires the separation of observed neurophysiological reactions into relevant components, confounding elements, and error terms. This procedure also includes the calculation of variance for each of these divisions, allowing the derivation of conclusions about the desired effects [54]. GLMs have a wide range of uses in various types of analysis, such as multiple regressions, one-sample t-tests, two-sample t-tests, analysis of variance (ANOVA), and analysis of covariance (ANCOVA). When concentrating on a single voxel, the GLM can be expressed in matrix form as:

$$y = X\beta + \epsilon \tag{2.4}$$

The observed response, denoted as the column vector y (with a scan length), is the result of a linear combination involving explanatory variables, often design effects or confounding. These variables are integrated into a design matrix X (with dimensions scans$\times$design variables). Accompanying this, there is an error vector ϵ (with a length equivalent to scans), which constitutes an independently and identically distributed Gaussian random component [54]. Each column within the design matrix is referred to as an explanatory variable, a regressor, or a covariate. The proportional impact of each of these columns on the observed response is represented in the column vector β (with a length corresponding to the design variables). These coefficients are derived through the use of a least squares method for estimation. Since explanatory variables can be categorised into design effects and confounders, a similar rationale is applied in defining the values β. The inferred variance of the parameter estimates is utilised to draw conclusions about them.

2.5.4.2 Statistical Inference: Drawing Meaning from Neuroimaging Data

An SPMT offers a means of assessing the null hypothesis that a specific linear combination, commonly referred to as a contrast, results in a value of zero for the estimates. The T statistic is computed by dividing the contrast or compound (determined by contrast weights) of the parameter estimates by the standard error of that compound. These contrasts enable the estimation of signal magnitudes concerning a singular condition, the disparity in magnitude between two conditions, or the collective magnitude average of multiple conditions. An SPMF facilitates the examination of the null hypothesis, where a matrix of contrast weights, comprising a composite of various T contrasts, equals zero. Each row in this matrix corresponds to one of the multiple simultaneous tests intended for evaluation [54].

Chapter 3

Literature Review

3.1 Social Behaviour in Healthy Controls: Oxytocin Impact

Investigations into the neural correlates of OT's effect on human social cognitive processes have been conducted through pharmacological fMRI studies. These studies discussed in this section, have followed double-blinded, placebo-controlled procedures, with all participants being male. Subjects were administered IN-OT at a dose of 24 to 32 IU [55].

The focus of these studies has been on the amygdala, as it plays a key role in human social cognition, particularly in the interpretation of facial expressions [56], and there is evidence of OT release and binding to the amygdala [57]. Animal studies have also suggested that the activation of OT receptors in the amygdala is related to the role of OT in social cognition, particularly in conspecific recognition [58].

In a pivotal study, subjects underwent an fMRI session under OT and placebo conditions while participating in a facial matching task that involved expressions of fear or anger. OT was found to reduce left amygdala activity when the subjects were exposed to negative emotional expressions on their faces. Furthermore, a reduction in the coupling between the amygdala and the brain stem was observed, which is critical for fear reactions [59]. This study established a crucial role for the amygdala in mediating OT's influence on social behaviour.

In a subsequent investigation, researchers expanded their focus to include positive-valence (happy) facial stimuli, broadening the scope beyond negative stimuli. OT was found to reduce amygdala reactivity to fearful and angry faces, as well as attenuate right amygdala activity associated with processing happy faces compared to neutral faces, suggesting that OT could reduce arousal to affective social stimuli in general by modulating amygdala activity [60]. However, laterality-specific effects have been observed, with OT reducing amygdala reactivity to happy faces mainly in the right hemisphere [60] and increasing amygdala activity primarily in the left hemisphere [4].

In general, these studies have provided insight into how OT influences neural activity during various aspects of social emotion processing through observation. However, it is important to note that human social interactions are heavily based on the information we acquire during interpersonal exchanges [61].

3.2 Social Behaviour in Schizophrenia: Oxytocin Impact

This dissertation builds on the findings of a previously conducted study [4] by incorporating individuals diagnosed with SCZ as an additional study population.

3.2.1 Endogenous Oxytocin

Animal models of schizophrenia have demonstrated that increasing endogenous OT levels can produce antipsychotic-like effects. For example, these treatments have been shown to reverse prepulse inhibition deficits induced by substances such as amphetamines [36]. Interestingly, individuals with SCZ often exhibit altered endogenous OT levels [62]. Generally, endogenous levels of OT in patients with SCZ tend to be lower compared to those of the healthy population [6], although conflicting findings have been reported in some studies [63–66].

Notably, research suggests that higher endogenous OT levels in patients with SCZ are associated with improved facial emotion recognition and social cognitive functioning [6]. On the contrary, lower endogenous OT levels have been predictive of poorer social cognitive functioning and deficits in the self-integration and metacognition domains [66, 67]. Furthermore, endogenous OT appears to affect nonsocial cognitive deficits, with lower levels associated with impaired processing speed and working memory [68, 69].

In general, OT appears to play a complex role in the pathophysiology of SCZ, affecting various symptom domains and cognitive functions. More research is needed to fully elucidate the mechanisms underlying these relationships.

3.2.2 Intranasal Oxytocin

In addition to studies that implicate endogenous OT in the pathophysiology of SCZ, there has also been progress in identifying the administration of IN-OT as a potential treatment option. Studies have been conducted that examine the effects of OT on the neural response to facial expressions in patients with SCZ [6].

For example, a single dose of 24 IU of IN-OT improved the ability of patients with SCZ to recognise most of the emotions presented to them [70]. Similarly, studies investigating fear recognition reported positive results [6, 71, 72], although some did not show significant differences between patients with SCZ and healthy controls [73]. It has also been explored whether 10 or 20 IU of IN-OT could reverse discrimination of impaired facial affect in patients with SCZ [72]. In particular, emotion recognition decreased in patients with SCZ after 10 IU of IN-OT, as they showed an increased tendency to identify all emotions, regardless of their actual presentation. On the other hand, emotion recognition improved after 20 IU of IN-OT in polydipsic patients compared to non-polydipsic patients [36].

Additionally, a single dose of IN-OT has been shown to enhance patients with SCZ performance in various cognitive social tasks, including deception detection, sarcasm recognition, emotion identification, and empathy [7]. Furthermore, it has been demonstrated to reduce both positive and negative symptoms in patients with SCZ [74].

Moreover, research has revealed IN-OT's ability to decrease amygdala activity in response to fearful emotions and increase in response to happy faces in patients with SCZ [6, 40]. In most studies with positive outcomes, IN-OT was administered at doses of 10 to 40 IU, except for a study by [71]. These results imply that OT has a differential modulatory effect on the amygdala responses to emotional faces when comparing patients with SCZ with healthy individ-

uals. However, several studies failed to demonstrate significant improvements in facial emotional recognition following OT treatment [75–77]. These studies are summarised in Table 3.1.

Study	Design and Dosing	Population	Results
Averbeck et al. 2011 [70]	dbRCT, crossover, 24 IU, single dose	21 SCZ	OT improved the ability of patients to recognise most emotions
Cacciotti-Saija et al. 2015 [75]	dbRCT, 24 IU twice daily, 6 weeks	52 SCZ	Nonsignificant facial emotion recognition task
Davis et al. 2013 [73]	dbRCT, 40 IU, single dose	24 SCZ	OT did not improve overall social cognition
Gibson et al. 2014 [71]	dbRCT, 24 IU twice daily, 6 weeks	14 SCZ	OT group increased fear recognition and perspective-taking
Goldman et al. 2011 [72]	dbRCT, crossover, 10 IU or 20 IU, single dose	13 SCZ, 5 PS, 8 NPS, 11 CTL	Emotional recognition decreased with 10 IU; improved with 20 IU around fear recognition in PS vs NPS
Horta de Macedo et al. 2014 [76]	dbRCT, crossover, 48 IU, single dose	28 SCZ, 20 CTL	Nonsignificant facial emotion task
Shin et al. 2015 [40]	dbRCT, crossover, 40 IU, single dose	16 SCZ, 16 CTL	OT decreased amygdala activity for fearful emotion and increased for happy
Strauss et al. 2018 [77]	dbRCT, 36 IU twice daily, 24 weeks	62 SCZ	Nonsignificant facial emotion recognition task

Table 3.1: Intranasal oxytocin treatment studies in patients with schizophrenia: effects on cognitive deficits. *Adapted from [6, 7].*

Chapter 4

Materials and Methods

This chapter covers the sample description and the methods adopted. Section 4.1 provides more demographic information about the sample data. Section 4.2 details the experimental protocol, as well as the fMRI paradigm. Section 4.3 outlines the methods of image acquisition. Finally, Section 4.4 explains the statistical analysis procedures.

4.1 Sample Description

Participants were recruited from the Instituto de Biofísica e Engenharia Biomédica (IBEB), University of Lisbon, at Hospital Júlio de Matos of Centro Hospitalar Psiquiátrico de Lisboa (CHPL). A prior study conducted by IBEB had already documented the demographics of the same sample used in this dissertation [78]. The research was approved by the CHPL review boards (Ref. CES005/2020) and endorsed by its scientific committee (Ref. CCP0031/2020). Data collection took place from June 1, 2020, to January 31, 2021, with all participants providing informed consent.

The inclusion criteria were men, native Portuguese speakers, right-handed, between 20 and 55 years old, with at least 4 years of education and a confirmed diagnosis of a psychotic disorder according to the International Classification of Diseases – 10th version (ICD-10), specifically SCZ (F20), persistent delusional disorder (F22), or schizoaffective disorder (F25), for at least 2 years and not before the age of 15. Participants were required to maintain a consistent psychiatric medication regimen for a minimum of 6 weeks and consent to blood samples, drug administration, and fMRI brain scanning. Additionally, as part of the preparation for the experiment, participants were instructed to abstain from alcohol and nicotine consumption for a period of 12 hours prior to the start of the study.

Exclusion criteria included recent hospitalisations related to psychiatric disease within the previous 2 months, use of illicit drugs within the past month, weekly alcohol consumption exceeding 28 units, prior diagnosis of significant neurological, hormonal, liver, gastrointestinal, infectious, cardiovascular, renal, or hematologic conditions, as well as a diagnosis of pervasive developmental disorders (ICD-10, F80-F89), colour blindness, history of traumatic brain injury with loss of consciousness, seizures, or premature birth (before the 37th week of gestation).

Initially, 64 participants were included in this project, however, 4 were excluded for being left-handed, 1 for excessive movement during preprocessing, and 3 for motion with a mean framewise displacement (FD) of 0.5mm or higher. For the statistical analysis, this left us with 56 subjects divided into three groups:

- Group 1 patients with SCZ who self-administered PBO (n=17);
- Group 2 patients with SCZ who self-administered IN-OT (n=18);
- Group 3 composed of healthy controls (n=21), with no history of mental illness, who self-administered PBO.

It is known that one group of patients with SCZ received PBO, while the other received OT. However, as will be elaborated on later, the specific allocation remains undisclosed to avoid any influence on the analysis.

4.2 Experimental Protocol

As discussed in Chapter 3, our project methods are similar to those of a previous study [4]. This was a double-blind, pseudo-randomised, placebo-controlled study, in which participants belonging to the SCZ-OT group received a single dose of 24 IU of OT (administered by Syntocinon spray, with three puffs per nostril, each containing 4 IU of Oxytocin), while the rest of the participants, SCZ-PBO and healthy controls, received a PBO spray containing all inactive components except the actual neuropeptide.

Previous research has shown that intranasally applied neuropeptides can cross the blood-brain barrier, providing a means to study the effects of OT on brain function [79]. OT or PBO was administered to participants approximately 45 minutes before the fMRI scan session, as OT levels of the central nervous system tend to stabilise around 40 minutes after substance administration [80]. The entire functional neuroimaging session did not exceed a duration of 13 minutes.

4.3 Imaging

4.3.1 Emotion Classification Paradigm

Participants performed a face emotion recognition task in which a male or female face expressing fearful, neutral, or happy emotions was presented in a pseudo-randomised and counterbalanced sequence in each of the three experimental sessions. The task required subjects to identify the emotion displayed on the screen, using their left thumb to answer fearful, the right thumb to answer neutral, and the right index to answer happy.

This event-related approach is different from the conventional "block design" method, in which the three face types are segregated into three distinct block sessions. In our approach, all face types are intermingled, and each individual trial is modelled. These ‘event-related’ and ‘pseudo-randomised’ trials give the impression of randomness, but the predetermined sequence for mixing emotions is actually preplanned in advance. There are four unique trial sequences, ensuring that no identical emotion or alignment is displayed consecutively more than three times and that the combination of the same emotion and alignment doesn’t occur more than two times in a row, as shown in Figure 4.1.

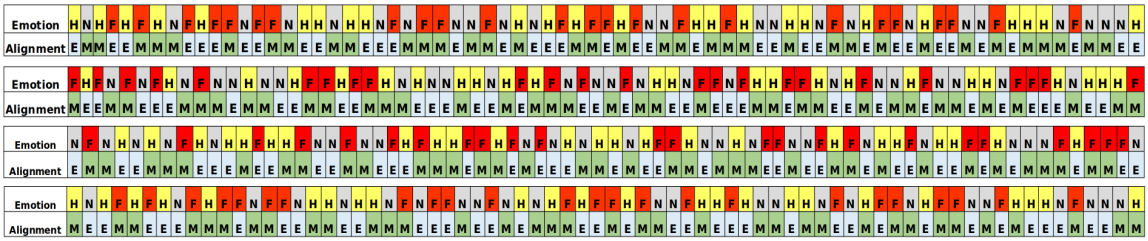

Figure 4.1: Schematic representation of 4 pseudo-randomised sequences balanced between groups and drugs. Emotion denotes the facial expression shown on screen (H, happy in yellow; N, neutral in grey; F, fearful in red) and Alignment is the main area focussed (E, eyes in light blue; M, mouth in green).

The experimental task used a fully crossed 3×2 within-subjects design, incorporating the variables of emotion and initial fixation. An fMRI session starts with 5 dummy scans to ensure that the magnetic field reaches a steady state before data acquisition. These scans were subsequently excluded from our calculations. Following the initial fixation cross (lasting 1 to 2 seconds), a facial image was displayed for 150 milliseconds. Subsequently, a blank screen persisted for 1,850 milliseconds, succeeded by a variable interstimulus interval, which could have a duration interval of from 2 to 9 seconds, during which participants could accurately identify the displayed emotion. This was succeeded by another fixation cross, maintained for a randomly determined period of 2 to 6 seconds (Figure 4.2). For precise regulation of the initial fixation, an unpredictable adjustment was implemented for half of the male and female stimuli associated with each emotional expression. This adjustment entailed shifting the stimuli either upward or downward on a per-trial basis, aligning the eyes or mouth with the position of the fixation cross. Neither the same emotion nor the same alignment was presented more than 2 times in succession.

Explicit decision-making was required in only 10% of the trials. During these trials, a screen displayed up to three words ("afraid," "neutral," and "happy") in the centre of the screen. Participants had a time limit of 3 seconds to respond. When they responded, a green square was drawn around their choice and remained for the remaining time within the 3-second limit. This explicit decision task was presented in only eight trials to introduce an element of unpredictability.

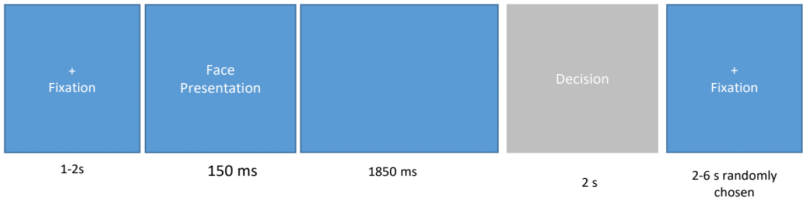

Figure 4.2: Schematic representation of the face valence design.

4.3.2 Image Acquisition

Data acquisition was performed using a Siemens Skyra 3T MRI system located at the CUF Tejo Hospital, employing a specialised 32-channel head coil for enhanced sensitivity and precision. The data collection process acquired a total of 403 volumetric samples, employing a $T_2{}^*$ echo-planar imaging (EPI) scan, known for its proficiency in capturing rapid changes in signal over time while maintaining spatial accuracy.

As part of this rigorous data collection effort, the imaging parameters were carefully defined through the implementation of an 80x80 matrix, which aligned seamlessly with a voxel size of

3mm isotropic. Temporal dynamics were effectively captured through a repetition time (TR) of 1960 ms, while an echo time (TE) of 30 ms was thoughtfully selected to optimise signal sensitivity. The choice of a 77° flip angle (FA) aimed to strike an optimal balance between signal strength and noise suppression. The field of view (FOV) was precisely delineated at 240 millimetres to ensure comprehensive spatial coverage.

Efficient multi-slice acquisition was facilitated by the application of a multiband interleaved ascending acquisition strategy across 56 slices. Notably, the phase encoding direction was meticulously defined as anterior to posterior, aligning with established anatomical standards and ensuring consistency in the acquired dataset.

Broadening the scope of this study, an additional high-resolution T1-weighted (T1w) anatomical image was acquired. This supplementary dataset employs a TR of 2200 milliseconds and a TE of 26 milliseconds. It should be noted that an inversion time of 900 milliseconds is included, a critical factor for optimal tissue contrast. The judicious selection of an 8° FA balanced signal intensity with potential radiofrequency energy deposition. The high-resolution nature of this acquisition was achieved through a matrix size of 288x288, harmonising with a voxel size of 0.8 millimetres isotropic. Comprising 192 slices, this imaging approach covered the anatomical volume in full.

4.3.3 Image Analysis

The functional volumes were preprocessed using *SPM12* (Wellcome Department of Imaging Neuroscience, Institute of Neurology, London, UK [81]), running on *MATLAB* 9.13.0.2080170 (R2022b) Update 1. The preprocessing workflow comprises five essential steps:

- Realignment: Occurs when the resulting images are aligned and spread out over a common reference point, usually the first volume of a sequence. The goal is to eliminate motion-related artefacts that may occur during scans [82, 83].
- Coregistration: Alignment of multiple image modalities obtained from the same subject. This ensures that the structural and functional images are precisely aligned in the same anatomical space, thereby maximising mutual information between the images [84].
- Segmentation: Structural images, such as T1w scans, are divided into grey matter (GM), white matter (WH), CSF, bone, soft tissue and background while generating deformation fields to transform subjects' brain shape into a reference brain [85].
- Normalisation: Maps each individual's brain data into a standardised coordinate space. This process allows group-level comparisons between subjects [82, 83].
- Smoothing: The spatial resolution of the images is reduced by applying a Gaussian filter, therefore increasing the signal-to-noise ratio (SNR) and reducing the effect of variability on the spatial location of functional regions between subjects [82, 83].

4.3.3.1 Anatomical Data Preprocessing

Anatomical data preprocessing was conducted using *fMRIPrep*, version 20.2.4, which builds upon the foundation of *Nipype*, version 1.6.1 [86, 87]. This preprocessing method has been previously established and is based on the *Nipype* framework [88,89]. Moreover, the preprocessing pipeline includes a series of analytical steps.

Previously acquired T1w images were first corrected for intensity non-uniformity (INU) using *N4BiasFieldCorrection* [48], a tool distributed within *ANTs* 2.3.3 [90]. The resulting corrected image served as a reference throughout the preprocessing pipeline. Subsequently, the T1w reference underwent skull-stripping using an implementation of the *antsBrainExtraction.sh* workflow (from *ANTs*) within *Nipype*, employing *OASIS30ANTs* as a target template.

Segmentation of CSF, WM, and GM was performed on brain-extracted T1w using the *fast* algorithm (*FSL* 5.0.9) [91]. Reconstruction of brain surfaces was achieved through the *recon-all* process (*FreeSurfer* 6.0.1) [92]. The previously estimated brain mask was refined using a custom variant of the method employed by *Mindboggle* to harmonise *ANTs*-derived and *FreeSurfer*-derived segmentation of cortical GM [93].

For volume-based spatial normalisation to the *MNI152NLin2009cAsym* standard space (ICBM 152 Nonlinear Asymmetrical template version 2009c) [94], a nonlinear registration approach was employed using the *antsRegistration* tool (*ANTs* 2.3.3). Both the T1w reference and the T1w template, subjected to brain extraction, were utilised in this registration process. The T1w template corresponds to the *MNI152NLin2009cAsym* standard space (TemplateFlow ID: MNI152NLin2009cAsym).

4.3.3.2 Functional Data Preprocessing

Initially, a reference volume and its skull-stripped counterpart were created using a customised approach implemented by *fMRIPrep*. To improve the quality of the data, five volumes were taken into account. A B0-nonuniformity map, also known as a field map, was calculated based on a phase difference map derived from a dual-echo GRE sequence (Gradient-recall Echo). The processing of this field map followed a tailored workflow inspired by the *epidewarp.fsl* script and incorporated advancements from HCP pipelines [95]. Subsequently, the field map was co-registered to the target EPI reference run and transformed into a displacement field map, which is compatible with registration tools such as *ANTs*, using *FSL*'s *fugue* and other *SDCflows* utilities. This field map was leveraged to compute a corrected EPI reference for improved co-registration accuracy with the anatomical reference.

Before any spatio-temporal filtering, head-motion parameters relative to the BOLD reference were estimated. This estimation included transformation matrices and their corresponding six rotation and translation parameters using *MCFLIRT* (*FSL* 5.0.9) [96]. Slice-time correction for BOLD runs was performed using *3dTshift* from *AFNI* 20160207 [97]. Afterwards, the BOLD time series, including slice-timing correction when applicable, were resampled back to their original, native space. This resampling was achieved by applying a composite transform designed to correct for both head motion and susceptibility distortions.

Following preprocessing in *fMRIPrep*, the preprocessed BOLD time series was further resampled in standard space, resulting in a preprocessed BOLD run aligned with *MNI152NLin2009c Asym* space at its native resolution (3 millimetres isotropic). For volume-based spatial coregistration with T1-space, *antsRegistration* (*ANTs* 2.4.4) and the *SyNBold* transform were employed. This transform combines an affine transformation with deformable adjustments, using mutual information as the optimisation metric. This process used brain-extracted versions of the T1w reference and a mean BOLD image derived from the raw BOLD data via *fslmaths*.

Various confounding time series were computed from the preprocessed BOLD data. Specifically, the calculation of the FD followed *Power's approach*, which involves summing the absolute relative motions, using the *Nipype* implementations [98].

In addition to FD, a set of physiological regressors was extracted to facilitate anatomical component-based noise correction (*aCompCor)* [99]. These *aCompCor* regressors were estimated following the "*aCompCor50% (24RP+aCompCor50%)*" pipeline [100]. First, probabilistic masks for CSF and WM were generated [99]. Before extracting principal components for each mask, the data were orthogonalised with respect to other variables included in the final regression model, namely, 24 motion parameters (translation, rotation, and their first and second derivatives), a bandpass filter within the range of 0.008-0.10 Hz, and a first-order polynomial. This preprocessing step ensured that the extracted principal components were optimally predictive. Lastly, spatial smoothing was applied using *AFNI*'s *3dBlurToFWHM*, employing an isotropic Gaussian kernel with a full-width half-maximum (FWHM) of 6 millimetres.

4.4 Statistical analysis

4.4.1 Performance Analysis

During the task, participants' performance was evaluated based on the number of questions answered and the speed of their responses. A higher level of performance is associated with a higher number of correct answers and shorter reaction times. It is important to note that reaction time was computed specifically for correct answers, and correct answers were calculated based on trials where subjects responded. In this analysis, the objective was to examine disparities between the groups with SCZ and to draw comparisons with the control group. Specifically, we aimed to assess whether the SCZ-PBO group exhibited a slower response time when compared to the SCZ-OT group. To achieve this, the data collected throughout the experiment were added to a `RESULTS_FILE.txt` file and processed using *Matlab*. Afterwards, analyses, including one-way ANOVAs and two-sample T-tests, were conducted in the *R* 4.3.1 environment.

4.4.2 Functional Brain Imaging Analysis

The statistical analysis of fMRI data in SPM employs a mass univariate approach based on GLMs. This statistical analysis process encompasses several key steps, including the definition of the GLM design matrix, the estimation of the GLM parameters using classical methods, and the hypothesis testing achieved through the creation of contrast vectors [82]. The GLM can be represented in matrix notation as follows:

$$Y = X\beta + \varepsilon, \quad \varepsilon \sim \mathcal{N}(0, \sigma^2 I) \tag{4.1}$$

In this context, Y represents the image data, with dimensions of scans$\times$voxels. The scans are collected over a specific time period, and all voxels form a three-dimensional image. X denotes the design matrix, with dimensions of scans$\times$design variables. β refers to the parameters that require estimation, with dimensions of design variables$\times$voxels. Lastly, ε represents an error matrix. It is postulated that this error matrix follows a normal distribution, characterised by a mean of 0 and a variance of σ^2, with the additional property that any two elements within the error term are uncorrelated [82].

4.4.2.1 First-level Analysis

In SPM, after preprocessing, the next step is model fitting. The objective is to estimate the BOLD level for each condition in every voxel of the brain. Consequently, the first-level analysis

generates contrast images for each condition.

A set of 12 regressors of interest, incorporating three emotions (Fearful, Happy, Neutral), two genders (Male, Female), and two fixation conditions (Mouth, Eyes), was utilised, along with their corresponding temporal derivatives. Additionally, three task-related regressors of no interest were incorporated, encompassing question presentation, left-finger responses, and right-finger responses, along with their respective temporal derivatives. The resulting design matrix is depicted in Figure 4.3. To account for potential sources of noise, 24 motion parameters were included, a bandpass filter within the frequency range of 0.008-0.10 Hz was applied, a 1st order polynomial was introduced, and noise regressors were derived from *aCompCor* components explaining 50% of the variance originating from both the CSF and WM masks.

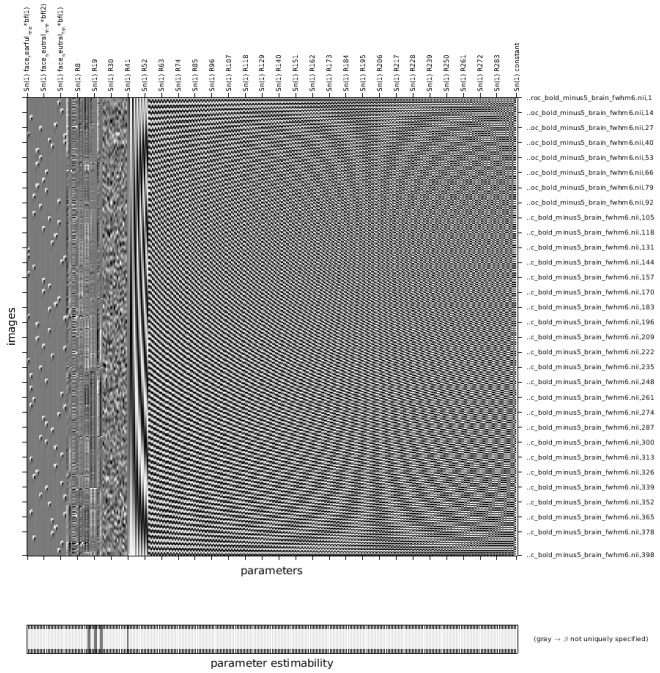

Figure 4.3: Single-level (1st level) design matrix, composed of 12 parameters of interest and 3 of no interest. The rows of the matrix are the individual functional scans obtained after preprocessing.

4.4.2.2 Second-level Analysis

For the group-level analysis, subject-specific contrast images were used in both the one-sample and two-sample T-tests. These analyses were conducted within *SPM*. Additionally, the drug condition (OT or PBO) were introduced to define distinct groups rather than serving as traditional regressors. The analysis involved direct group-to-group comparisons. For instance, the Fearful, Happy, and Neutral contrasts represent the estimation of activation evoked by all fearful, happy, and neutral image presentations, respectively. These contrasts were utilised in the analysis to capture the neural responses associated with each specific emotion.

A one-sample T-test is performed to determine whether the mean values of contrast images, obtained individually from a group of subjects, significantly differ from a reference value, typically zero (Figure 4.4). This analysis is not subject-specific in the sense of examining each individual's results but rather evaluates if the effects within the contrast images, specific to individual subjects, collectively deviate significantly from zero within a single group. In essence, there is a comparison of the group's contrast images to this reference value of zero to identify statistically significant deviations.

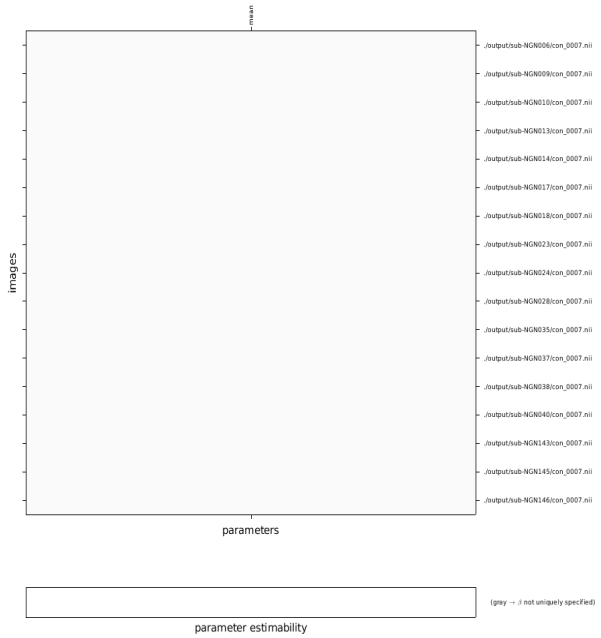

Figure 4.4: Group level (2^{nd}-level) design matrix of Group 1 for condition 7 (fearful emotion) for One-sample T-test.

Afterwards, a two-sample T-test was used to facilitate the comparison of activation maps between two distinct groups of subjects. The contrast images for each group were inputted and the mean activation and variance for each voxel were estimated. This procedure generated two statistical T maps and contrast images that showed regions where significant differences in mean activation were observed between the two groups (Figure 4.5). To account for the variation of activation peak across subjects, the analysis was conducted on slightly smoothed contrast images (FWHM = 5 millimetres).

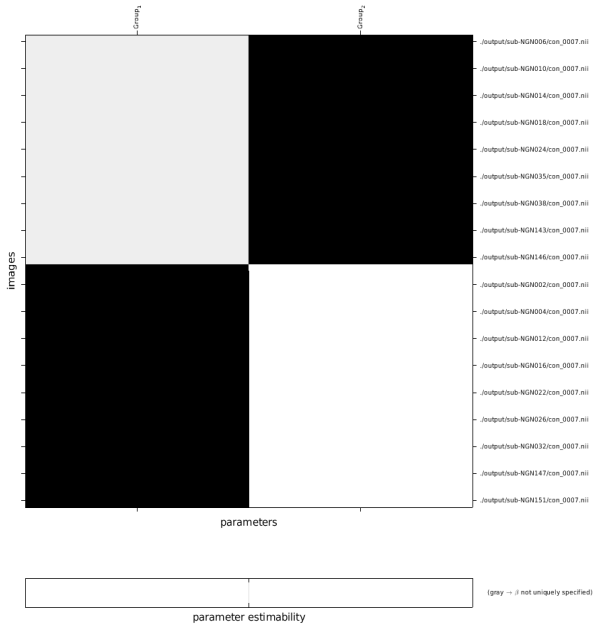

Figure 4.5: Group level (2^{nd}-level) design matrix of Group 1 vs Group 2 for condition 7 (fearful emotion) for Two-sample T-test.

4.4.3 Region of Interest Analysis

Subsequently, these data undergo analysis within the *R* environment. This approach differs from the voxel-based method employed in *SPM*, which assumes uniform peak coordinates across subjects. In contrast, the current method is structured to extract data in a manner that accommodates variations in activation among individuals, ultimately leading to a reduction in the number of statistical tests.

The data extraction process is comprised of several steps. Firstly, the voxels of the given contrast image that pertain to the specified sphere ROI are selected. Next, a minimal threshold of T=1, derived from the T-map, is applied. Finally, the voxels belonging to a putative peak, typically defined as the top X% of the remaining activated voxels (for instance, 5% as used in our analysis), are identified. Subsequently, the values from this set of voxels are averaged [101].

This reduction aligns with the concept of 'small volume correction' in *SPM*, which involves fewer tests compared to exploring the entire brain voxel by voxel.

The primary objective is to obtain a value for each subject that optimally characterises their individual activation within a designated ROI. Four distinct ROIs were utilised in the analysis:

- A spherical ROI with a radius of 3 millimeters and center coordinates (-28, -4, -28), as derived from [4].
- A Gamer et al. (2010) Superior Sphere ROI with coordinates x=-27, y=-2, z=-17 millimeters and a radius of 2 voxels [4].
- A Gamer et al. (2010) Inferior Sphere ROI with coordinates x=-23, y=-3, z=-28 millimeters and a radius of 2 voxels [4].
- An atlas-defined ROI from AAL3, specifically number 45.

Initially, a spherical ROI with coordinates derived from [4], was employed. Subsequently, following the methodology employed in the aforementioned study, these spherical ROIs were subdivided to explore potential areas of heightened activation. It was considered that different parts of the amygdala may react differently to oxytocin administration, as demonstrated by [4]. This subdivision resulted in a reduction of voxels within the ROIs while enhancing the specificity of the analysis with respect to neural regions. Moreover, all of these regions of interest are located within the left amygdala, as no statistically significant findings were reported in this specific anatomical region [4].

Furthermore, the incorporation of the Automated Anatomical Labelling (AAL3) atlas was deemed appropriate due to its improved anatomical precision, potentially enabling the detection of activations that might not be evident when using the spherical ROI alone. However, it should be noted that this precision could lead to the potential oversight of some individual variations in activation patterns, particularly in cases of substantial variability in peak activation locations across subjects.

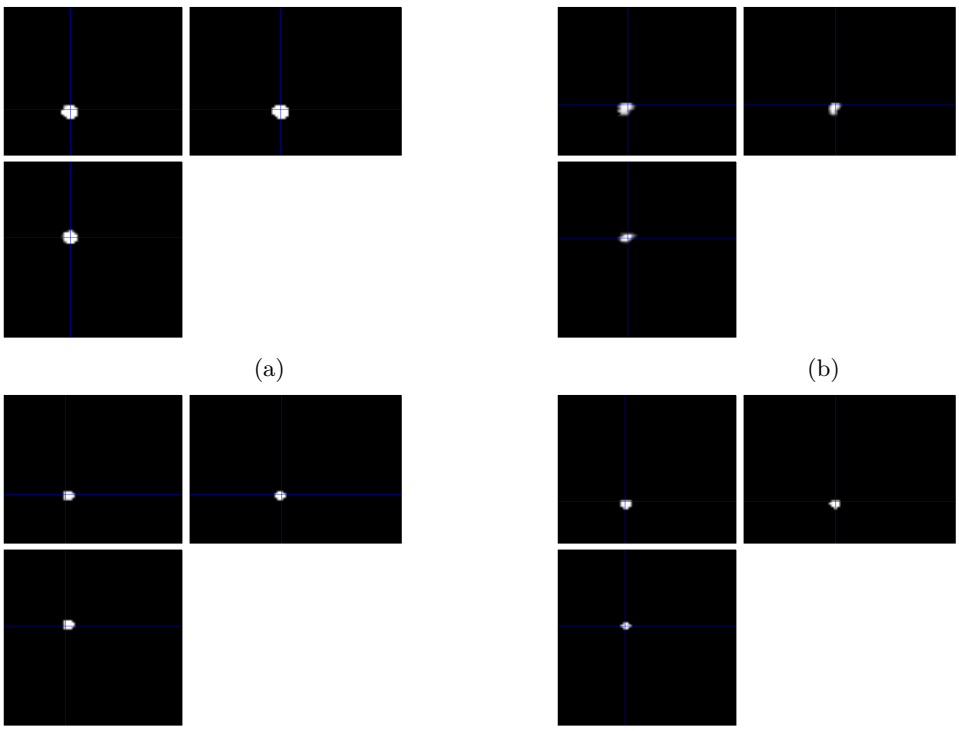

Figure 4.6: Display of the four different regions of interest. (a) Sphere ROI, coordinates x=-28, y=-4, z=-28 millimetres with a radius of 3 voxels. (b) Atlas ROI from AAL3, number 45. (c) Gamer Superior Sphere ROI, coordinates x=-27, y=-2, z=-17 millimetres with a radius of 2 voxels [4]. (d) Gamer Inferior Sphere ROI, coordinates x=-23, y=-3, z=-28 millimetres with a radius of 2 voxels [4].

In *R*, the model included the variables listed in Table 4.1. We examined the individual influence of each predictor variable on the dependent variable by performing a main effects analysis. This type of analysis looks at the change in the dependent variable associated with a one-unit change in the predictor variable while keeping all other predictors constant. For categorical predictor variables with more than two levels, the main effect assesses the difference in the mean of the dependent variable between the reference category and each of the other categories. This helps to understand how each category affects the dependent variable relative to the reference category. Main effects provide insights into the individual impact of each predictor variable on the dependent variable while considering the other predictors in the model. They are essential for understanding the relationships between the predictors and the outcome variable and are usually reported alongside interaction effects, if present, in regression analysis to give a comprehensive understanding of the model's results.

Afterwards, we conducted nested models in our analysis. This is a series of regression models in which each successive model either includes or excludes certain predictor variables or interaction terms from the previous model. The purpose of this is to compare the fit of the nested models and determine if the inclusion of certain variables or interactions significantly improves the model's performance. We began with a full linear regression model that included a three-way interaction term: [OT] x Group x Emotion. We then created reduced models by excluding specific interaction terms or main effects and examined the impact of individual two-way interaction terms ([OT] x Group, [OT] x Emotion, Group x Emotion). We used ANOVA to compare the full model with the reduced models. The ANOVA results provided p-values that indicated whether the exclusion of specific terms significantly affected the model's fit. By

comparing different models with progressively fewer predictor variables or interaction terms, we were able to assess the significance of these terms in explaining the variation in the dependent variable.

Variable	**Description**
Amygdalar Activation	Quantitative continuous dependent variable
[OT]	Quantitative continuous independent variable
Group	Categorical independent variable
Emotion	Categorical independent variable

Table 4.1: Variables used in the statistical model and their description.

Chapter 5

Results and Discussion

In this chapter, the outcomes of the techniques elucidated in Chapter 4 are presented and comprehensively discussed as we progress through the chapter. The performance analysis of the subjects is shown in Section 5.1, followed by the results of the ROI analysis in Section 5.2. Finally, the results of the model analysis are presented in Section 5.3.

5.1 Performance Analysis

This analysis sought to determine if there were any significant differences in response time and accuracy of answers between two groups of people with SCZ. Table 5.1 shows the mean and standard deviation (SD) of reaction time and the total good answer rate, which is the ratio of correct answers to total answers. As discussed in Section 3.2.2, people with SCZ have difficulty recognising facial expressions. Therefore, it was hypothesised that the SCZ-OT group would perform more similarly to healthy controls than the SCZ-PBO group.

As part of the task, participants were given a 3-second window to indicate the emotion corresponding to the face presented. However, some subjects were excluded due to either their lack of response or responses submitted after the allotted time, resulting in a slightly different list as presented in Section 4.1.

- Group 1 patients with SCZ who self-administered PBO (n=13);
- Group 2 patients with SCZ who self-administered IN-OT (n=15);
- Control composed of healthy controls (n=20).

		Group 1	**Group 2**	**Control**
Mean Reaction Time (ms)	**Mean**	1060.465	1010.251	905.291
	SD	344.801	362.277	235.380
Total Good Answer Rate (%)	**Mean**	79.386	89.722	94.911
	SD	26.977	13.875	8.599

Table 5.1: Mean and standard deviation (SD) of mean reaction time and correct answers' rate (Total Good Answer and Total Good Answer Rate, respectively) by diagnostic group.

The graphs below in Figure 5.1 are a visual representation of the information presented above by Table 5.1.

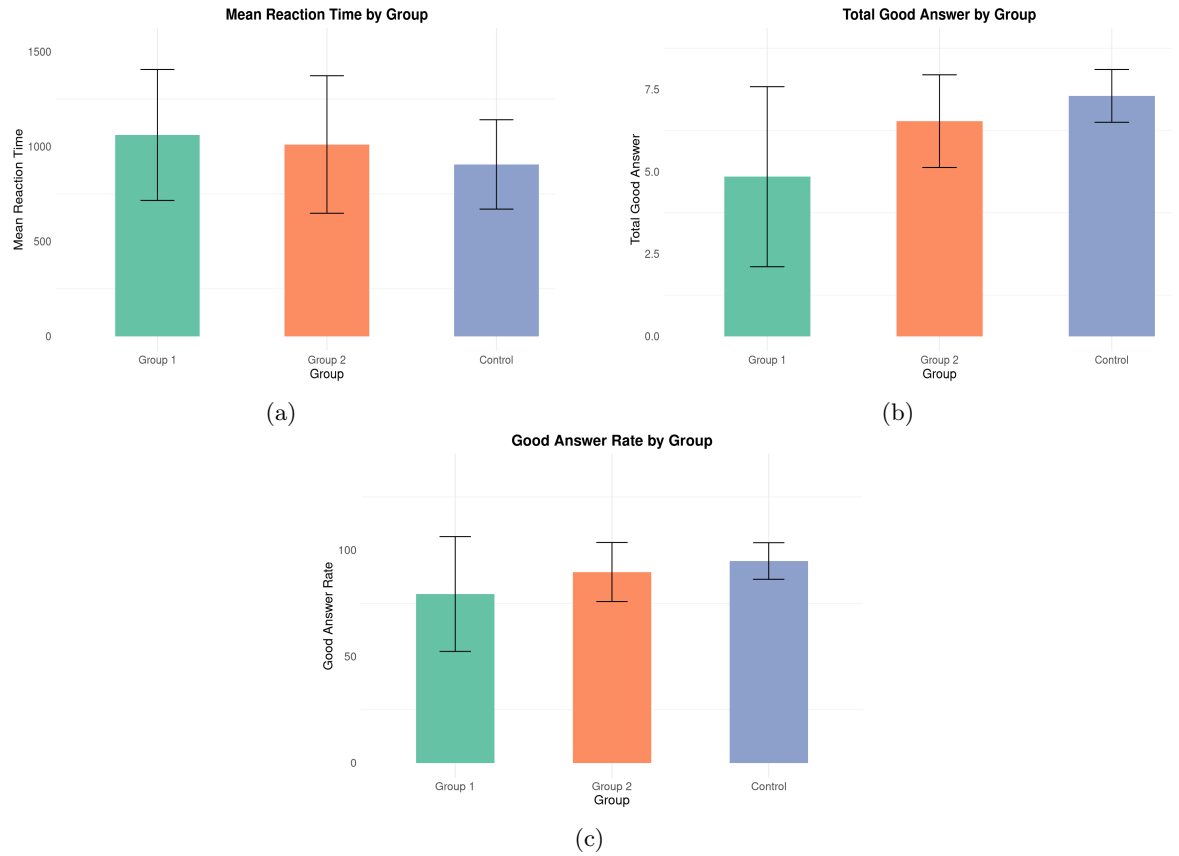

Figure 5.1: Bar charts between Group 1 (green), Group 2 (orange) and control (blue). The corresponding means and standard deviation are shown in Table 5.1. (a) Bar chart of the mean response time of each group. (b) Bar chart showing the average number of correct answers for each group. (c) Bar chart of the rate of correct responses between the groups.

In general, it can be observed that Group 1 had a satisfactory response rate of approximately 79.4%, indicating that 79.4% of their responses were in agreement with the correct emotional expression. On the other hand, Group 2 showed a notable increase of 89.7%. It is important to note that the average of non-responses was computed as well. Group 1 had 39% and Group 2 had 24% of non-responses rate. This reveals that Group 1 provided fewer responses, of which 79.4% were deemed correct. Conversely, Group 2, despite a higher number of responses, achieved a correct response rate of 89.7%.

Although there were minor disparities in the average reaction times among the groups, these distinctions, albeit existent, are relatively modest. Specifically, Group 1 exhibited an average reaction time of around 1060.5 milliseconds, while Group 2 demonstrated a slightly quicker average reaction time of 1010.3 milliseconds. It is noteworthy to mention that these distinctions may not carry significant practical consequences for comprehending the variances in emotional expression processing speed across the groups.

When comparing Group 1 with the control, there is a stark difference in both their mean reaction times and total good answer rate. Control has a mean response time of 905.291 milliseconds and approximately 94.9% total good answer rate. These results are aligned with previous studies exploring these relationships on facial emotion recognition which have also found shorter response times for the control group [102–106] and a higher average score on emotion

recognition [106].

Based on the statistical tests outlined in Table 5.2, it becomes evident that although differences were observed in the investigated variables, not all of these differences reached statistical significance. For the variable of mean reaction time, neither the one-way ANOVA nor the two-sample t-test yielded statistically significant results. Consequently, one can conclude that there is no significant difference in mean reaction times between the three groups. Specifically, for Group 1 and Group 2, the mean reaction times of these two groups are similar.

Regarding the variable of total good answers, the one-way ANOVA showed a significant result ($p < 0.001$), indicating differences in the mean scores among the three groups. However, further examination using a two-sample t-test revealed that the difference between Group 1 and Group 2 was marginally significant ($p = 0.061$). Although the difference did not reach conventional significance levels ($p < 0.05$), it suggests a potential trend or a trend toward a difference. It is, however, between Group 1 and Control that exhibits statistical significance with a p-value of 0.007.

In accordance with prior literature [106], the relationship between Group 1 and the Control group is congruent. Nevertheless, unlike that study, a reduced sample size is employed, resulting in a diminished level of statistical power. Therefore, the attainment of an adequate level of statistical power was not guaranteed by our sample size. To address this concern, a sensitivity test should be employed to calculate the minimum required effect size. Additionally, a noteworthy limitation lies in the high rate of non-response, which impedes an accurate estimation of cognitive abilities in perceiving emotion among SCZ patients, given that reaction time and the average number of correct answers were computed only for trials with responses, thereby excluding unsuccessful trials. Therefore, confidence in the actual task performance of the subjects is constrained by this limitation. Another improvement that could be made is dividing the mean reaction time and total good answers by emotion since it has been shown that SCZ individuals have better results for happy faces [107].

	One-way ANOVA		**Two-sample T-test**		
	F-value (Df)	**p-value**	**Interaction**	**t-statistic (Df)**	**p-value**
Mean Reaction Time	1.092 (2, 45)	0.344	**G1 vs G2**	0.375 (25.746)	0.711
			G1 vs CTL	1.422 (19.255)	0.171
			G2 vs CTL	0.978 (22.599)	0.339
Total Good Answer	8.306 (2, 45)	$<0.001^{***}$	**G1 vs G2**	-2.007 (25.746)	0.061
			G1 vs CTL	-3.149 (13.351)	0.007^{**}
			G2 vs CTL	-1.892 (20.732)	0.073

Table 5.2: One-way ANOVA results for Mean Reaction Time and Total Good Answer by Group (F-value and p-value). Two-sample T-test results for Mean Reaction Time and Total Good Answer between Groups (t-statistic and p-value). Abbreviations: Df, degrees of freedom; Group 1, G1; Group 2, G2; CTL, control.

5.2 Functional Brain Imaging Analysis

The data in this section will be conveyed via a table, commonly accompanied by a visual representation of the regions where an effect was observed. In this visual representation, colour

bars will be used to indicate the magnitude of the T-value. he voxels that passed the initially defined significance threshold of 0.05, either in a voxel-level FWE corrected or uncorrected manner (for images without corrected results), with no minimal cluster, along with the maximal activation peak coordinates, the peak T-value, and the cluster abbreviations linked to anatomical descriptions validated using the anatomical human atlas [108].

The methods outlined in Section 4.4.2 are initially employed by beginning with a one-sample T-test on individual groups.

The aim of the one-sample T-test is to ascertain the regions associated with the task of facial recognition for contrast fearful, happy and neutral, within the entire sample, utilising a p-value of 0.05 FWE corrected while refraining from imposing a minimum cluster extent (0 voxels).

The paradigm was found to be associated with the activation of several brain regions, including the right crus I of cerebellar hemisphere, left and right lobule VI of the cerebellar hemisphere, right inferior temporal gyrus and left superior frontal gyrus, orbital part for Group 1, as indicated in Table 5.3 and Figure 5.2. In the case of the other groups, activation within those regions was also observed (as detailed in Appendix A).

All of these regions have been associated with the emotion recognition process, such as the right crus I of the cerebellar hemisphere [109]. In particular, the left lobule VI was associated with difficulties in perceiving neutral and fearful faces in healthy individuals [110]. In SCZ, studies have found that individuals seem to have structurally smaller temporal lobe volume compared with healthy controls [111, 112].

Fearful				
	Peak MNI Coordinates			
T-value	**x (mm)**	**y (mm)**	**z (mm)**	**Cluster Labelling**
8.25	44	-58	-22	Cerebelum_Crus1_R
7.28	**38**	**-60**	**-24**	Cerebelum_6_R
Happy				
	Peak MNI Coordinates			
T-value	**x (mm)**	**y (mm)**	**z (mm)**	**Cluster Labelling**
7.51	**-28**	**-54**	**-18**	Cerebelum_6_L
7.50	48	-72	-4	Temporal_Inf_R
Neutral				
	Peak MNI Coordinates			
T-value	**x (mm)**	**y (mm)**	**z (mm)**	**Cluster Labelling**
7.76	**-16**	**32**	**-20**	Frontal_Sup_Orb_L

Table 5.3: Significant regions at $p<0.05$ FWE corrected, for the effect of the different emotions during Face Emotion Recognition Task on Group 1. The coordinates in bold represent the nearest local maximum represented in Figure 5.2. Abbreviations (from AAL3): Cerebelum_Crus1_R, right crus I of the cerebellar hemisphere; Cerebelum_6_R, right lobule VI of the cerebellar hemisphere; Cerebelum_6_L, left lobule VI of the cerebellar hemisphere; Temporal_Inf_R, right inferior temporal gyrus; Frontal_Sup_Orb_L, left superior frontal gyrus, orbital part.

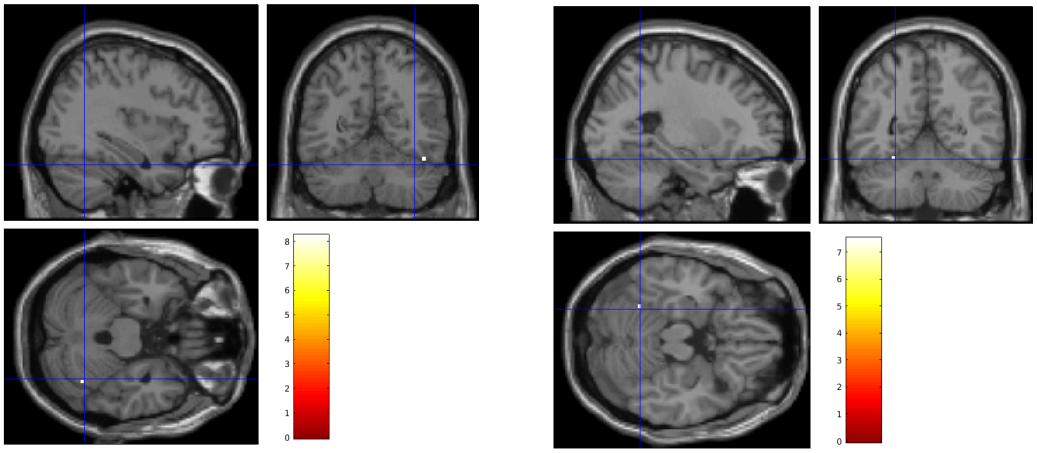

(a)

(b)

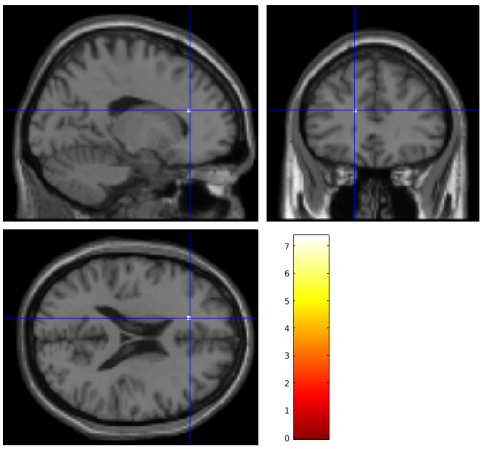

(c)

Figure 5.2: Sagittal, Axial, and Coronal Slices of the significant regions at FWE corrected for the positive effect on the Fearful, Happy and Neutral contrast in Group 2 during the Face Emotion Recognition Task. There is little to no activation in all regions (colour bars indicate T-values). The blue cross represents the nearest local maximum with its coordinates in bold in Table 5.3. (a) Activation for Fearful contrast (p=0.046, 0 cluster, corrected), displayed on an anatomical slice (x=38, y=-60, z=-24) in the right lobule VI of the cerebellar hemisphere. (b) Activation of Happy contrast (p=0.031, 0 cluster, corrected), displayed on an anatomical slice (x=-28, y=-54, z=-18) in the left lobule VI of the cerebellar hemisphere. (c) Activation for Neutral contrast (p=0.040, 0 cluster, corrected), displayed on an anatomical slice (x=-16, y=32, z=-20) in the left superior frontal gyrus, orbital part.

However, a significant level of activation is notably absent, and no activation is observed within the amygdalar area. Nonetheless, the analysis proceeded to the two-sample T-test, where significant results could not be obtained, even with a significance threshold set at $p = 0.05$ uncorrected and without a minimal cluster size. It is worth noting that while the T-test did not yield statistically significant results for most comparisons, there was a marginally significant T-value of 0.051 observed for group 1 compared to group 2 in the fearful contrast within this analysis. This finding suggests a subtle difference between groups in the context of fear, although it falls just beyond the conventional significance threshold.

These results of both one-sample and two-sample T-test could be due to the first-level analysis model, where the number of covariates, including frequency filtering and movement regressors, was primarily reduced, while the original number of experimental conditions remained unchanged. Importantly, modifications were made to the threshold for masking, and it is plausible that this

adjustment in the masking threshold contributed to the subsequent absence of the amygdala region in the analysis. Additionally, it should be noted that this may also influence the region of interest analysis in Section 5.3. This influence may extend to activation levels, despite the fact that this analysis is not voxel-based; it still relies on the outcomes of the first-level analysis.

5.3 Region of Interest Analysis

In the absence of notable findings throughout Section 5.2, it is opportune to transition into a discussion about the *SPM* ROI analysis approach. It should be noted that the *SPM* ROI analysis operates on a voxel-based methodology. Consequently, the use of a custom script for ROI data extraction results in a dataset with a reduced emphasis on precise anatomical localisation. This unique feature sets the stage for the subsequent statistical analysis conducted in *R*, as elaborated upon in the following sections.

5.3.1 Endogenous Oxytocin

The endogenous level of OT of each participant was measured before the start of the experience. This measurement involved obtaining blood samples, specifically measuring plasma OT concentrations, which allowed for the determination of baseline OT levels in the participants. The upcoming section explores the relationship between endogenous [OT] with amygdalar activation.

5.3.1.1 Analysis of Sphere ROI

To visualise the association between endogenous [OT] and left amygdala activation within the ROI Sphere, the graphs presented in the following figures were plotted.

Figure 5.3 illustrates a nearly parallel trend between the groups, suggesting a similar relationship between [OT] (the independent variable) and activation of the left amygdala (the dependent variable) at different levels of the group. Therefore, there may be no significant interaction effect.

On the other hand, Figures 5.4 and 5.5 display intersecting lines, particularly noticeable between Group 1 and Group 2. These intersections indicate the presence of an interaction effect. They imply that the influence of the independent variable ([OT]) undergoes changes in direction or magnitude, at varying levels of the dependent variable (Left amygdala activation).

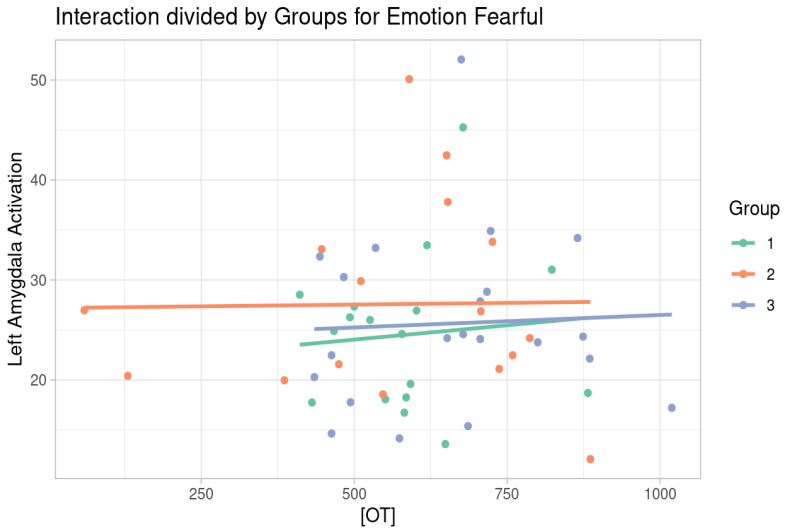

Figure 5.3: Scatterplot depicting the relationship between Left Amygdala Activation (Sphere ROI, coordinates x=-28, y=-4, z=-28 millimetres [4]) and the concentration of endogenous OT ([OT]) for Fearful emotions, divided by Group 1 (green), Group 2 (orange), and Group 3 or Control (blue).

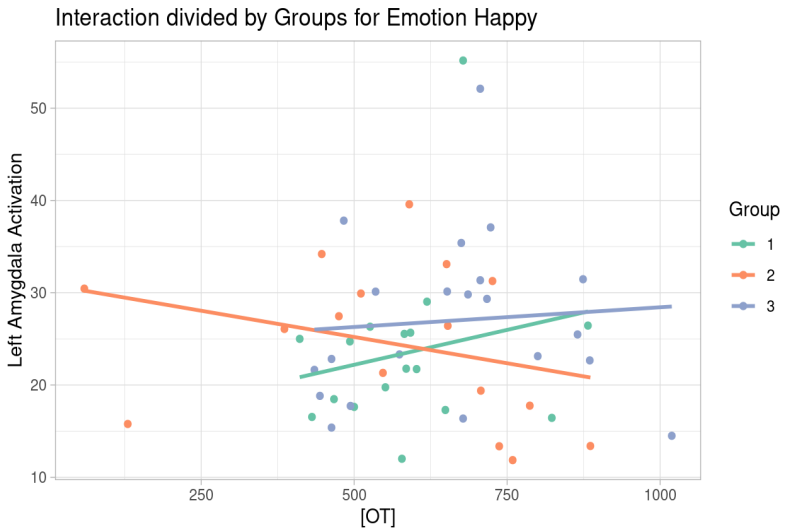

Figure 5.4: Scatterplot depicting the relationship between Left Amygdala Activation (Sphere ROI, coordinates x=-28, y=-4, z=-28 millimetres [4]) and the concentration of endogenous OT ([OT]) for Happy emotions, divided by Group 1 (green), Group 2 (orange), and Group 3 or Control (blue).

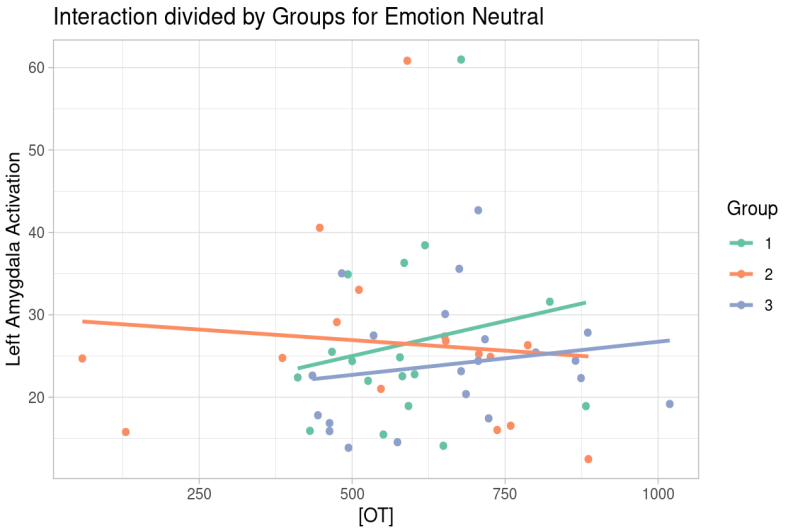

Figure 5.5: Scatterplot depicting the relationship between Left Amygdala Activation (Sphere ROI, coordinates x=-28, y=-4, z=-28 millimetres [4]) and the concentration of endogenous OT ([OT]) for Neutral emotions, divided by Group 1 (green), Group 2 (orange), and Group 3 or Control (blue).

However, upon further statistical analysis detailed in Section 4.4.3, a more comprehensive interpretation of the relationships between endogenous [OT], Group, Emotion, and left amygdala activation was provided.

The main effects of [OT], Group and Emotion were assessed individually with all of them obtaining a p-value > 0.05: p-value for [OT] 0.765, Group 0.765 and Emotion 0.921. Suggesting that these variables do not demonstrate a significant main effect on left amygdala activation for this region.

Additionally, their interaction effects also yield non-significant results. The three-way interaction effect between [OT] x Group x Emotion showed a p-value of 0.913 which indicated the influence of [OT] on the left amygdala activation does not significantly change in direction, strength, or magnitude across different groups and emotion conditions. Moreover, interaction effects between [OT] x Group and [OT] x Emotion also returned non-significant p-values of 0.959 and 0.949, respectively, further cementing that the relationship between [OT] and left amygdala activation remains consistent across different groups and emotion conditions.

Similarly, the interaction effect Group x Emotion showed a non-significant result with a p-value of 0.941, indicating that the relationship between Group and Emotion does not significantly affect left amygdala activation.

Main Effects	t-value	p-value
[OT]	0.300	0.765
Group	0.268	0.765
Emotion	0.082	0.921
Interaction Effects	**F (Df)**	**p-value**
[OT] x Group x Emotion	0.498 (12)	0.913
[OT] x Group	0.439 (14)	0.959
[OT] x Emotion	0.466 (14)	0.949
Group x Emotion	0.465 (13)	0.941

Table 5.4: Statistical Results of the Interaction Effects of Endogenous Oxytocin ([OT]), Group, and Emotion on Left Amygdala Activation (Sphere ROI, coordinates x=-28, y=-4, z=-28 millimetres [4]) during the Facial Emotion Recognition Task. Abbreviations: Df, degrees of freedom.

5.3.1.2 Analysis of Gamer et al. (2010) Superior Sphere ROI

The division of the Sphere ROI into two sections was executed based on the coordinates extracted from the study conducted by [4]. This section refers to the coordinates of the left superior amygdala, shown in Figure 5.6. In the process of subdividing and subsequently narrowing the analysed area, a reduction in participants' data was observed. In this particular case, data on the amygdalar activation of two participants (one belonging to Group 2 and the other to the Control group) were not within the delineated region, reducing our participants' number to 54 for fearful emotions.

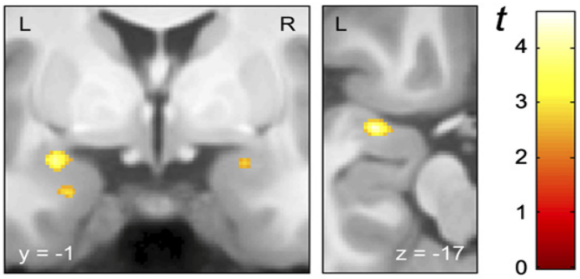

Figure 5.6: Amygdala regions showing a significant interaction of group and emotional expression. (Right) Statistical map (coronal and axial plane) of the interaction effect revealing two clusters in the left amygdala (superior cluster, peak voxel: x=27, y=2, z=17 millimetres; and inferior cluster, peak voxel: x=23, y=3, z=28 millimetres). *Adapted from [4].*

The graphs below show a visual representation of the relationship between [OT] and left amygdala activation within the ROI Gamer Superior.

Figures 5.7, 5.8 and 5.9 display predominantly intersecting lines between groups in varying slopes, indicating the presence of an interaction effect (except in Figure 5.8 between Group 2 and Control). This implies that the influence of [OT] undergoes changes in direction or magnitude, at varying levels of the left amygdala activation variable.

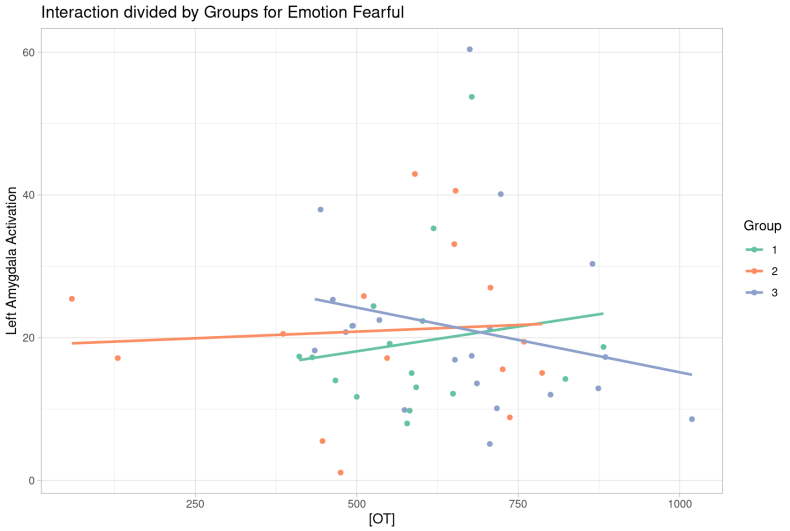

Figure 5.7: Scatterplot illustrating the relationship between Left Amygdala Activation (Gamer et al. (2010) Superior Sphere ROI, coordinates: x=-27, y=-2, z=-17 millimetres [4]) and the concentration of endogenous OT ([OT]) for Fearful emotions, with data points categorized by Group 1 (green), Group 2 (orange), and Group 3 or Control (blue).

Figure 5.8: Scatterplot illustrating the relationship between Left Amygdala Activation (Gamer et al. (2010) Superior Sphere ROI, coordinates: x=-27, y=-2, z=-17 millimetres [4]) and the concentration of endogenous OT ([OT]) for Happy emotions, with data points categorized by Group 1 (green), Group 2 (orange), and Group 3 or Control (blue).

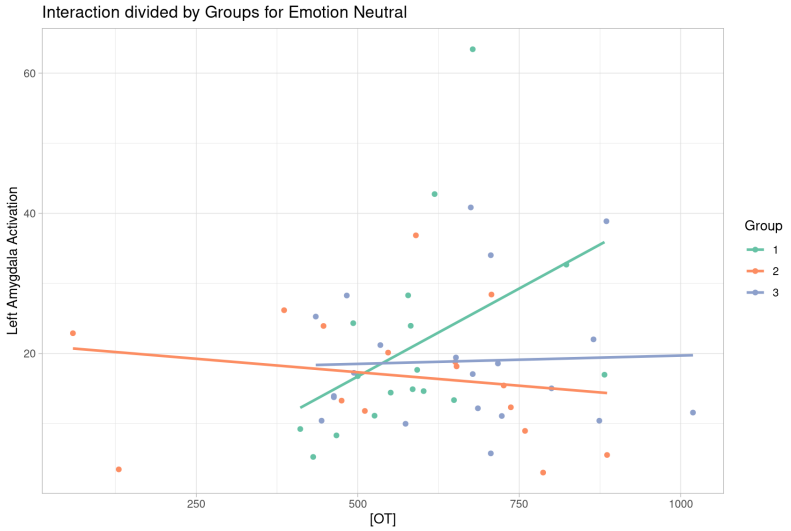

Figure 5.9: Scatterplot illustrating the relationship between Left Amygdala Activation (Gamer et al. (2010) Superior Sphere ROI, coordinates: x=-27, y=-2, z=-17 millimetres [4]) and the concentration of endogenous OT ([OT]) for Neutral emotions, with data points categorized by Group 1 (green), Group 2 (orange), and Group 3 or Control (blue).

Nonetheless, no statistical significance was found for the main and interaction effects of the variables (Table 5.5).

The results of the main effects of [OT], Group and Emotion had a p-value > 0.05, implying no statistically significant effect in this region. For [OT] the p-value was 0.539, Group 0.839 and Emotion 0.719. Furthermore, the interaction effects also showed no significant results with p-values for the three-way interaction of 0.569, [OT] x Group of 0.667, [OT] x Emotion of 0.691 and Group x Emotion of 0.644, all above 0.05.

In general, as in the previous region, these results present a consistent relationship between [OT] and left amygdala activation remains across different groups and emotions.

Main Effects	**t-value**	**p-value**
[OT]	0.616	0.539
Group	0.175	0.839
Emotion	0.330	0.719
Interaction Effects	**F (Df)**	**p-value**
[OT] x Group x Emotion	0.880 (12)	0.569
[OT] x Group	0.801 (14)	0.667
[OT] x Emotion	0.779 (14)	0.691
Group x Emotion	0.814 (13)	0.644

Table 5.5: Statistical Results of the Interaction Effects of Endogenous Oxytocin ([OT]), Group, and Emotion on Left Amygdala Activation (Gamer et al. (2010) Superior Sphere ROI, coordinates: x=-27, y=-2, z=-17 millimetres [4]) during the Facial Emotion Recognition Task. Abbreviations: Df, degrees of freedom.

5.3.1.3 Analysis of Gamer et al. (2010) Inferior Sphere ROI

The preceding Section 5.3.1.2 delved into the coordinates of the superior left amygdala, whereas this section will focus on the coordinates of the inferior left amygdala shown in Figure 5.6. As mentioned above, in the process of subdividing and subsequently narrowing the analysed area, a reduction in the participants' data was observed; in this case, more subjects were excluded. A total of five levels of activation of the left amygdala were removed from the analysis. Reducing the participants' number to 54 for fearful emotions, 54 for happy emotions, and 55 for neutral emotions.

The graphs below pertaining to Figures 5.10, 5.11, and 5.12 do not show a significant interaction effect, as they represent a nearly parallel trend between the groups.

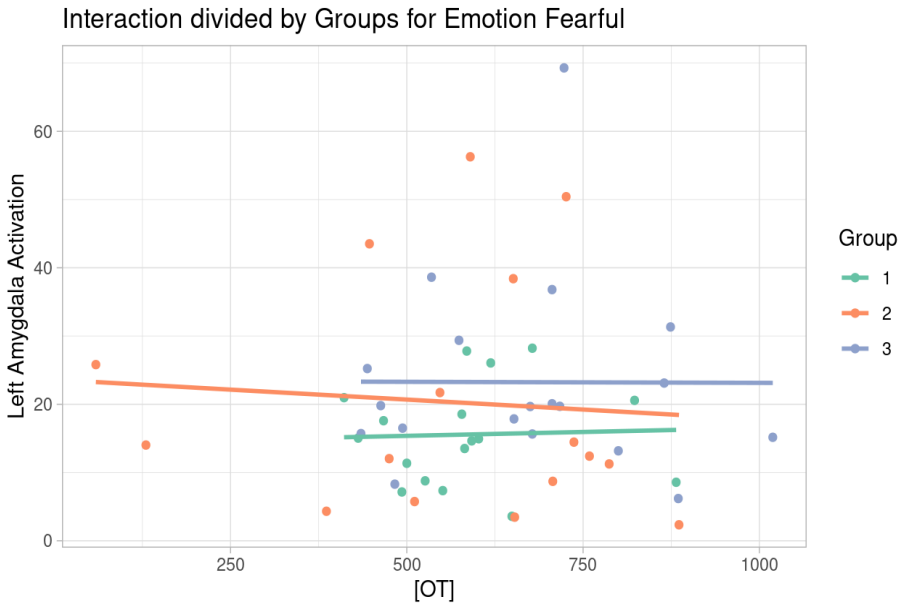

Figure 5.10: Scatterplot illustrating the relationship between Left Amygdala Activation (Gamer et al. (2010) Inferior Sphere ROI, coordinates: x=-23, y=-3, z=-28 millimetres [4]) and the concentration of endogenous OT ([OT]) for Fearful emotions, with data points categorized by Group 1 (green), Group 2 (orange), and Group 3 or Control (blue).

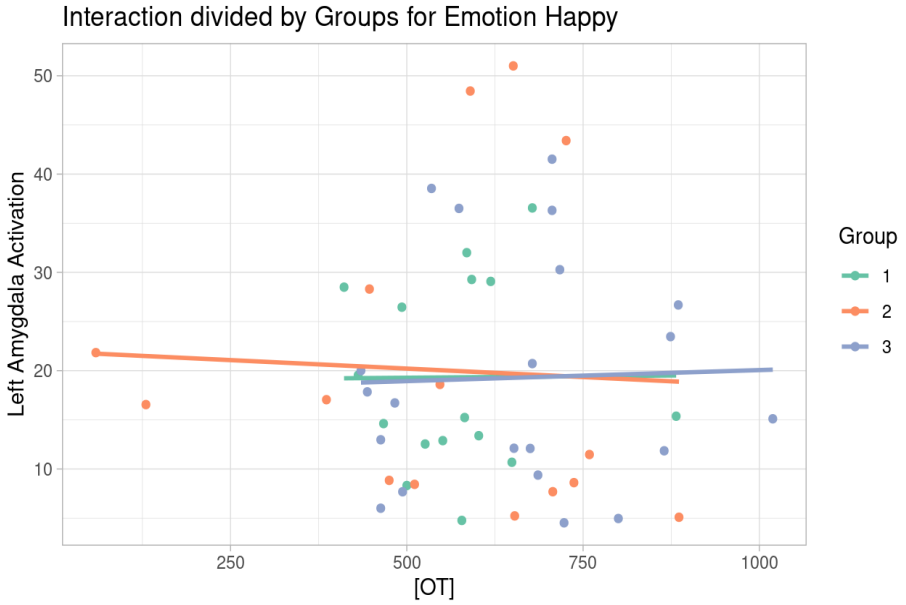

Figure 5.11: Scatterplot illustrating the relationship between Left Amygdala Activation (Gamer et al. (2010) Inferior Sphere ROI, coordinates: x=-23, y=-3, z=-28 millimetres [4]) and the concentration of endogenous OT ([OT]) for Happy emotions, with data points categorized by Group 1 (green), Group 2 (orange), and Group 3 or Control (blue).

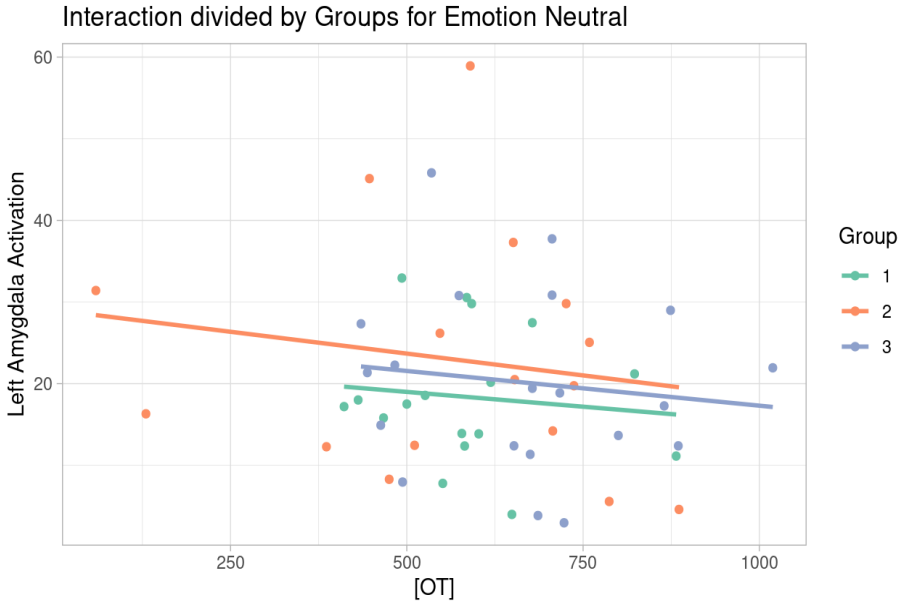

Figure 5.12: Scatterplot illustrating the relationship between Left Amygdala Activation (Gamer et al. (2010) Inferior Sphere ROI, coordinates: x=-23, y=-3, z=-28 millimetres [4]) and the concentration of endogenous OT ([OT]) for Neutral emotions, with data points categorized by Group 1 (green), Group 2 (orange), and Group 3 or Control (blue).

Maintaining the prevailing pattern, there were no statistically significant results of these variables' interactions and main effects. In Table 5.6, for all main effects the p-value is > 0.05 meaning it did not find strong evidence to reject the null hypothesis. Likewise, the interaction effects continue to exhibit no significant results with p-values of 0.997, 0.999, 0.983 and 0.997, for the three-way interaction, [OT] x Group, [OT] x Emotion and Group x Emotion, respectively. In fact, these p-values are closer to 1.0 meaning that there is very little evidence against the null

hypothesis.

Main Effects	t-value	p-value
[OT]	0.088	0.930
Group	1.171	0.313
Emotion	0.078	0.925
Interaction Effects	**F (Df)**	**p-value**
[OT] x Group x Emotion	0.225 (12)	0.997
[OT] x Group	0.204 (14)	0.999
[OT] x Emotion	0.361 (14)	0.983
Group x Emotion	0.248 (13)	0.997

Table 5.6: Statistical Results of the Interaction Effects of Endogenous Oxytocin ([OT]), Group, and Emotion on Left Amygdala Activation (Gamer et al. (2010) Inferior Sphere ROI, coordinates: x=-23, y=-3, z=-28 millimetres [4]) during the Facial Emotion Recognition Task. Abbreviations: Df, degrees of freedom.

5.3.1.4 Analysis of AAL3 ROI

The analysis of the AAL3 ROI is subsequently conducted, affording an anatomically precise representation of the left amygdala. No participant data is excluded, thereby ensuring the inclusion of all 56 participants within these results.

The subsequent graphs depict intersecting lines, portraying an accentuated slope between Group 1 and Group 2 for all three emotions, possibly suggesting a noteworthy relationship between them (Figures 5.13, 5.14 and 5.15).

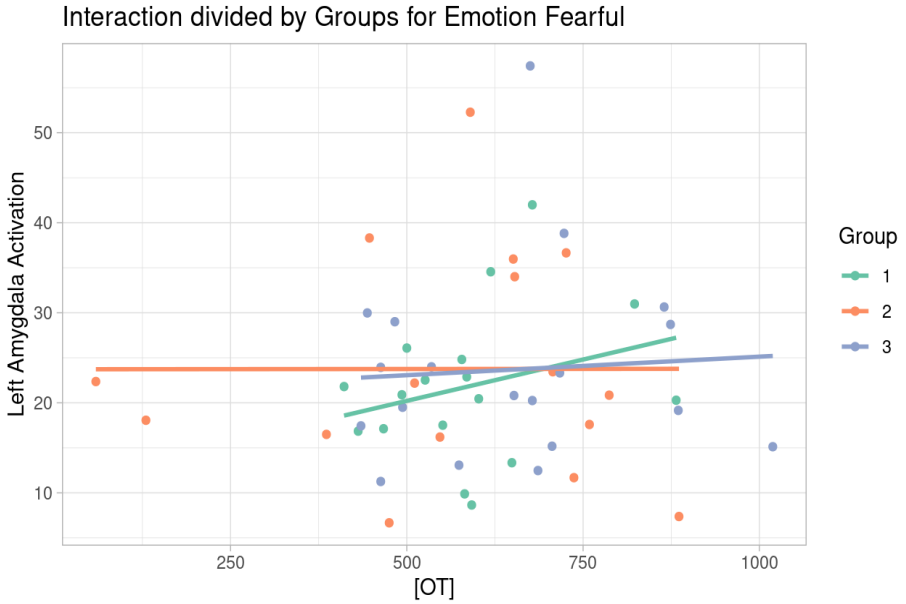

Figure 5.13: Scatterplot depicting the relationship between Left Amygdala Activation (AAL3 ROI, number: 45) and concentration of endogenous OT ([OT]) for Fearful emotions, divided by Group 1 (green), Group 2 (orange), and Group 3 or Control (blue).

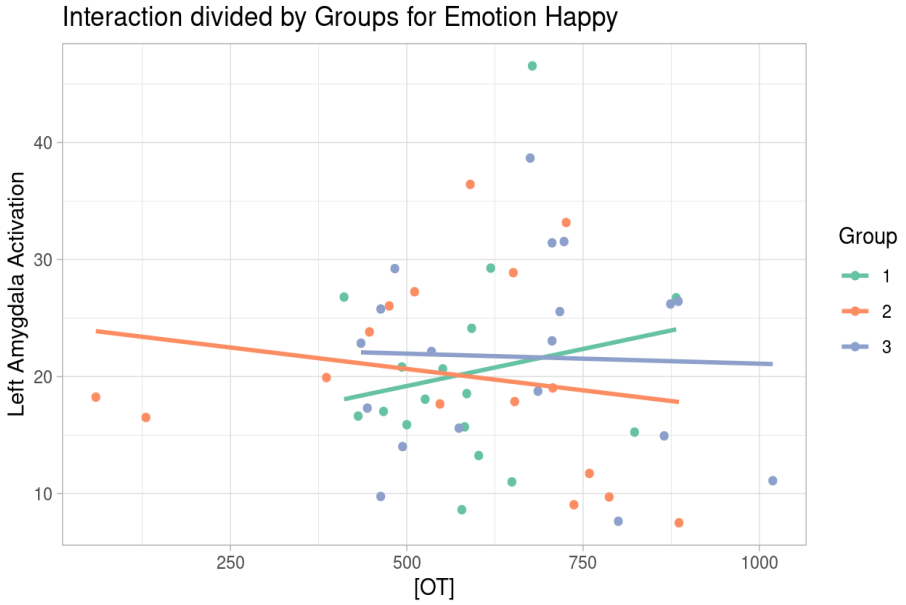

Figure 5.14: Scatterplot depicting the relationship between Left Amygdala Activation (AAL3 ROI, number: 45) and concentration of endogenous OT ([OT]) for Happy emotions, divided by Group 1 (green), Group 2 (orange), and Group 3 or Control (blue).

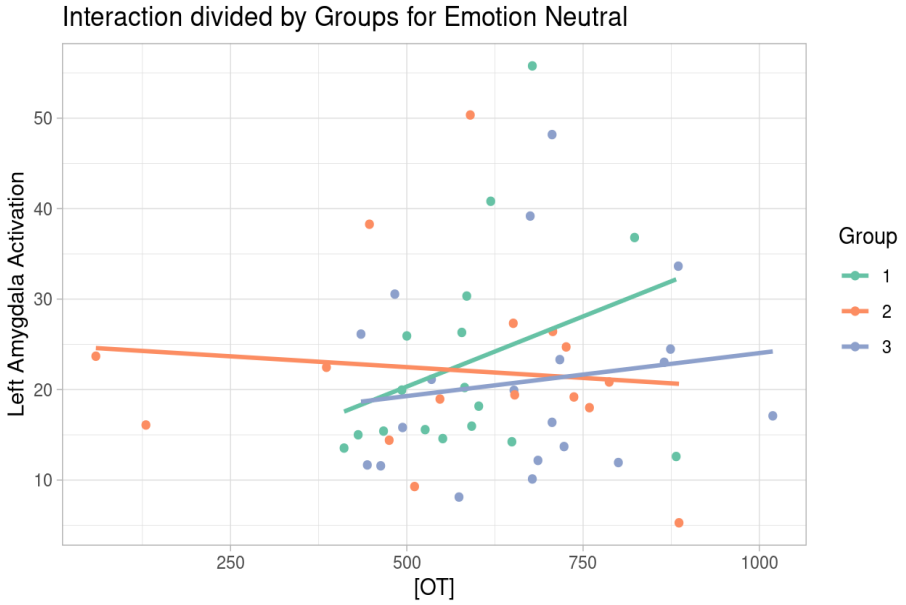

Figure 5.15: Scatterplot depicting the relationship between Left Amygdala Activation (AAL3 ROI, number: 45) and concentration of endogenous OT ([OT]) for Enutral emotions, divided by Group 1 (green), Group 2 (orange), and Group 3 or Control (blue).

However, when looking at the statistical tests presented in Table 5.7, no significant results are observed for either the main effects or the interaction effects. Specifically, there are p-values that closely approach 1.0, indicating a scarcity of evidence supporting the rejection of the null hypothesis.

Regarding the main effects, the p-values are 0.376, 0.983, and 0.596 for [OT], Group, and Emotion, respectively. Meanwhile, for the main effects, [OT] x Group x Emotion exhibits a p-value of 0.939, [OT] x Group has a p-value of 0.950, [OT] x Emotion has a p-value of 0.976, and Group x Emotion has a p-value of 0.953.

Main Effects	t-value	p-value
[OT]	0.887	0.376
Group	0.017	0.983
Emotion	0.520	0.596
Interaction Effects	**F (df1, df2)**	**p-value**
[OT] x Group x Emotion	0.451 (12)	0.939
[OT] x Group	0.461 (14)	0.950
[OT] x Emotion	0.389 (14)	0.976
Group x Emotion	0.440 (13)	0.952

Table 5.7: Statistical Results of the Interaction Effects of Endogenous Oxytocin ([OT]), Group, and Emotion on Left Amygdala Activation (AAL3 ROI, number: 45) during the Facial Emotion Recognition Task.

Overall, the results exposed throughout Section 3.2.1 and its subsections, revealed no significant interactions were observed in any of the regions. However, throughout the analysis, graphical interactions occasionally indicated a greater degree of similarity between the SCZ-OT group and the control group (Figures 5.3, 5.8, and 5.12).

Mixed results have been reported when investigating the role of endogenous OT in SCZ. The predominant approach involves assessing peripheral OT levels as an indicator of central OT function. However, as stated before this study uses plasma OT. Its use as a surrogate for central OT remains unconfirmed as plasma OT levels can be influenced by peripheral organs such as the heart, gastrointestinal tract, and reproductive organs [113]. Nevertheless, it is worth noting that positive correlations have been observed [64, 114].

In [64], a positive correlation was identified in a sample of 40 individuals with schizophrenia. The study employed dynamic tasks consisting of videos featuring male and female actors portraying various emotions, including happiness, sadness, neutrality, and anger. Research has indicated that dynamic videos elicit a stronger response in individuals compared to static photographs [115], a finding that could be considered for implementation in this study.

5.3.2 Intranasal Oxytocin

In the following section, the relationship between IN-OT concentration and amygdala activity will be examined. After the initial measurement of OT, some participants did not undergo a second measurement of OT, resulting in their exclusion from this analysis.

- Group 1 patients with SCZ who self-administered IN-OT (n=17);
- Group 2 patients with SCZ who self-administered PBO (n=17);
- Group 3 composed of healthy controls (n=19), with no history of mental illness, who self-administered PBO.

5.3.2.1 Analysis of Sphere ROI

The graphs below show a visual representation of the relationship between IN-[OT] and left amygdala activation for the Sphere ROI. Figures 5.16, 5.17 and 5.18 all display intersecting

lines between groups for fearful, happy and neutral emotions, respectively. This interaction suggests that the relationship between IN-[OT] and emotional responses is not uniform, but varies depending on the level of activation of the left amygdala.

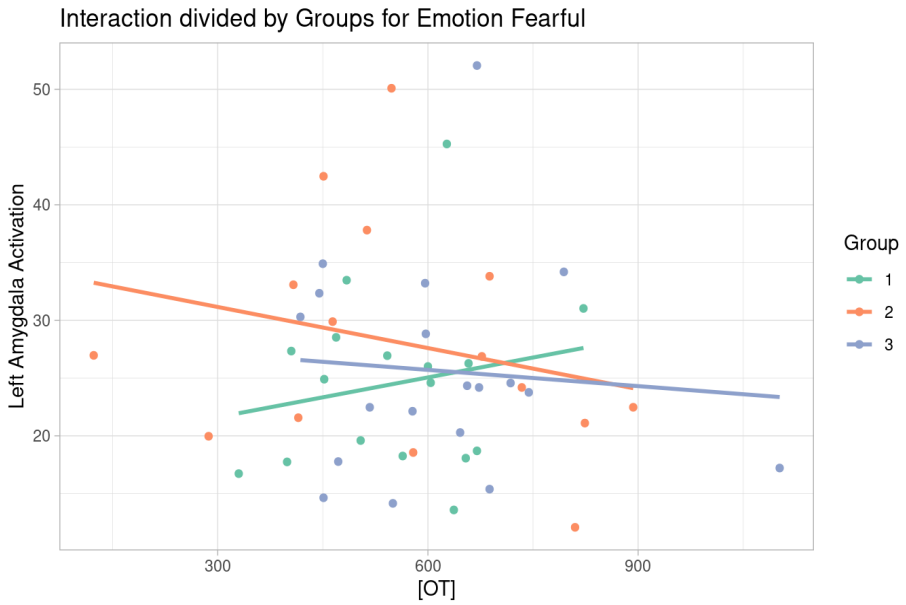

Figure 5.16: Scatterplot depicting the relationship between Left Amygdala Activation (Sphere ROI, coordinates x=-28, y=-4, z=-28 millimetres [4]) and concentration of IN-OT ([OT]) for Fearful emotions, divided by Group 1 (green), Group 2 (orange), and Group 3 or Control (blue).

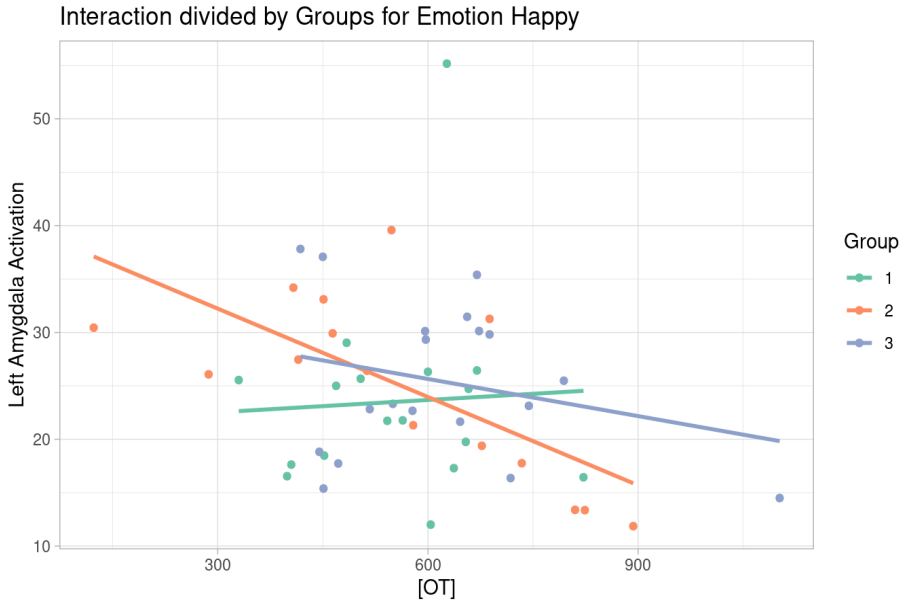

Figure 5.17: Scatterplot depicting the relationship between Left Amygdala Activation (Sphere ROI, coordinates x=-28, y=-4, z=-28 millimetres [4]) and concentration of IN-OT (IN-[OT]) for Happy emotions, divided by Group 1 (green), Group 2 (orange), and Group 3 or Control (blue).

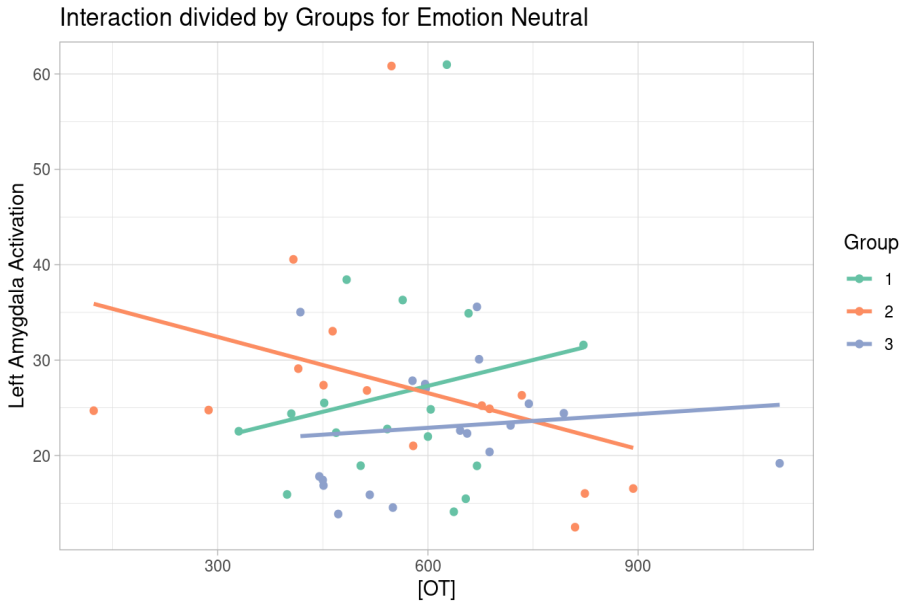

Figure 5.18: Scatterplot depicting the relationship between Left Amygdala Activation (Sphere ROI, coordinates x=-28, y=-4, z=-28 millimetres [4]) and concentration of IN-OT (IN-[OT]) for Neutral emotions, divided by Group 1 (green), Group 2 (orange), and Group 3 or Control (blue).

However, it's important to note that this interaction does not demonstrate statistical significance, as indicated by the results presented in Table 5.8. Each of the main effects of [OT], Group, and Emotion was assessed individually, and in each case, the p-value exceeded 0.05. Specifically, the p-value for [OT] and Group was 0.765, and for Emotion, it was 0.921. This suggests that these variables do not exhibit a significant standalone effect on left amygdala activation in this particular region.

Furthermore, the interaction effects between these variables also yielded non-significant results. The three-way interaction effect between [OT] x Group x Emotion produced a p-value of 0.913, indicating that the influence of [OT] on left amygdala activation does not significantly vary in terms of direction, strength, or magnitude across different groups and emotional conditions. Additionally, the interaction effects between [OT] x Group and [OT] x Emotion returned p-values of 0.959 and 0.948, respectively, further confirming that the relationship between [OT] and left amygdala activation remains consistent across different groups and emotional states.

Similarly, the interaction effect between Group x Emotion showed a non-significant result with a p-value of 0.941, suggesting that the relationship between Group and Emotion does not significantly impact left amygdala activation.

Main Effects	t-value	p-value
[OT]	0.300	0.765
Group	0.268	0.765
Emotion	0.082	0.921
Interaction Effects	**F (Df)**	**p-value**
[OT] x Group x Emotion	0.451 (12)	0.939
[OT] x Group	0.498 (12)	0.913
[OT] x Emotion	0.439 (14)	0.959
Group x Emotion	0.466 (13)	0.948

Table 5.8: Statistical Results of the Interaction Effects of Intranasal Oxytocin (IN-[OT]), Group, and Emotion on Left Amygdala Activation (Sphere ROI, coordinates x=-28, y=-4, z=-28 millimetres [4]) during the Facial Emotion Recognition Task. Abbreviations: Df, degrees of freedom.

5.3.2.2 Analysis of Gamer et al. (2010) Superior Sphere ROI

In accordance with a study conducted by [4], the Sphere ROI was divided into two distinct regions for analysis. It was observed that, for some participants, their data points extended beyond the defined boundaries of these delineated regions. Consequently, the data from these participants were excluded from the analysis. It is worth noting that in addition to the participants who were initially excluded from the study, data from two more subjects, one from Group 2 and another from the Control group, were also omitted from the analysis specifically related to the analysis of fearful emotions.

In the graphical representation displayed below, we can observe intersecting lines among different Groups, as illustrated in Figures 5.19, 5.20, and 5.21. However, it's worth noting that in Figure 5.20, the Control group and Group 2 exhibit a parallel trend, suggesting the absence of a significant relationship between these two groups.

Nevertheless, intersecting interactions, represent critical junctures in the data, signifying instances where the relationships depicted by these variables undergo noteworthy changes.

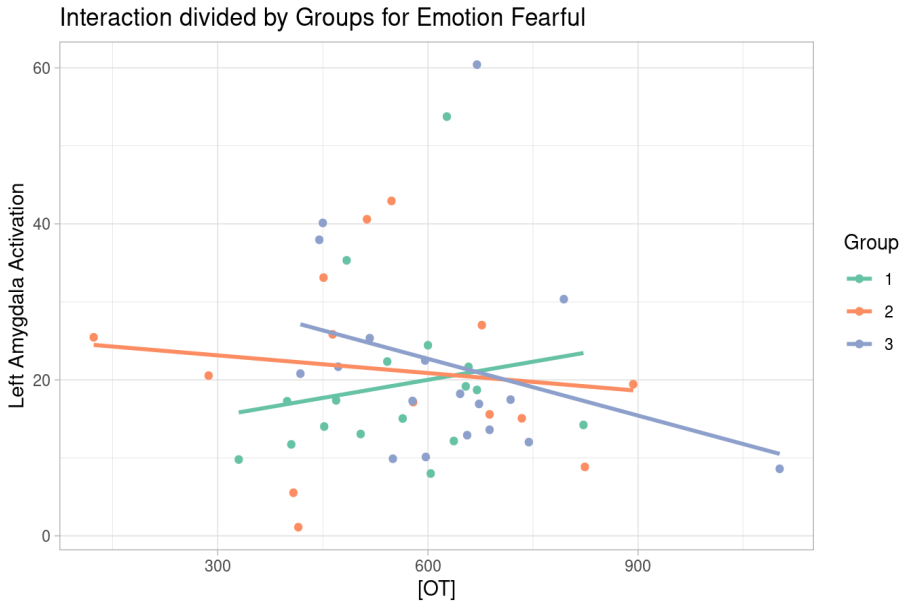

Figure 5.19: Scatterplot depicting the relationship between Left Amygdala Activation (Gamer et al. (2010) Superior Sphere ROI, coordinates: x=-27, y=-2, z=-17 millimetres [4]) and concentration of IN-OT (IN-[OT]) for Fearful emotions, divided by Group 1 (green), Group 2 (orange), and Group 3 or Control (blue).

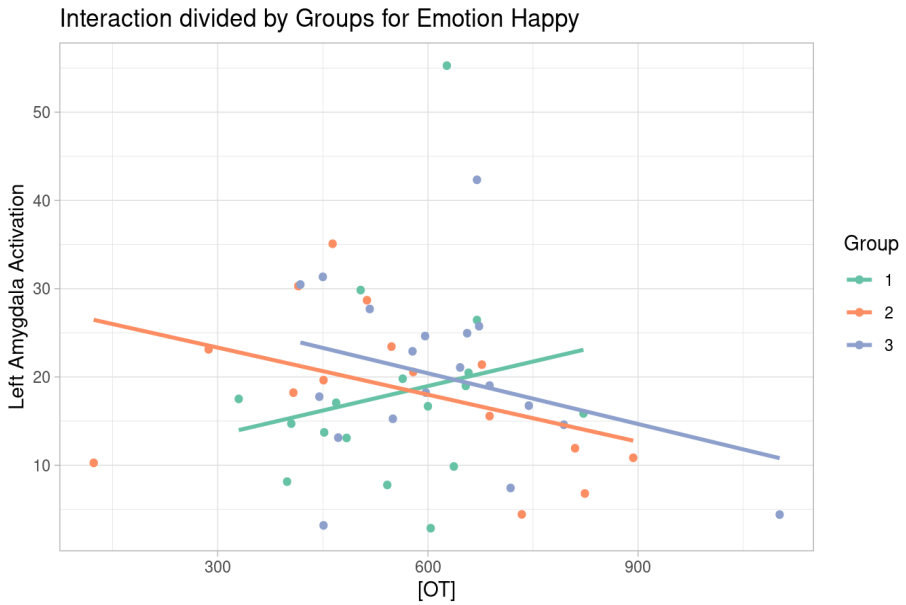

Figure 5.20: Scatterplot depicting the relationship between Left Amygdala Activation (Gamer et al. (2010) Superior Sphere ROI, coordinates: x=-27, y=-2, z=-17 millimetres [4]) and concentration of IN-OT (IN-[OT]) for Happy emotions, divided by Group 1 (green), Group 2 (orange), and Group 3 or Control (blue).

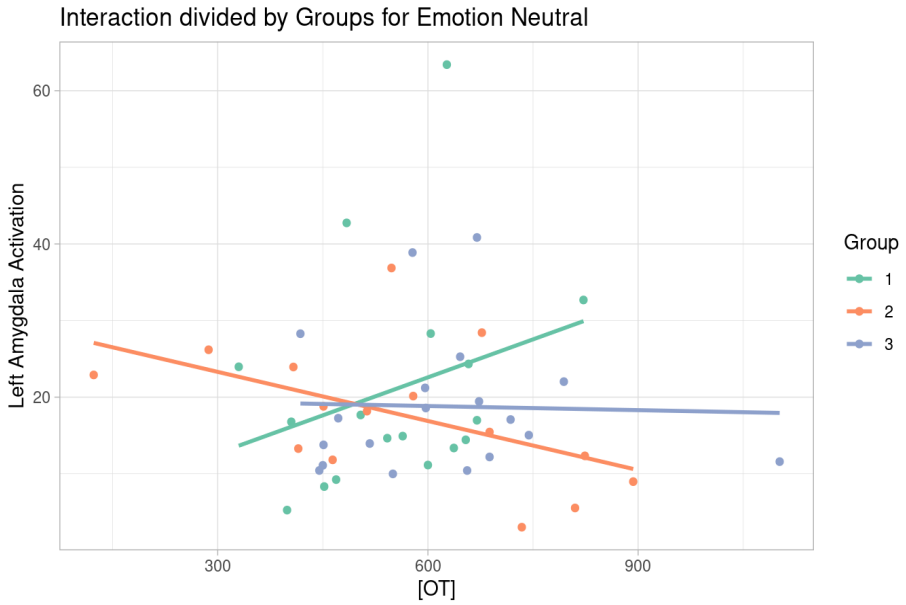

Figure 5.21: Scatterplot depicting the relationship between Left Amygdala Activation (Gamer et al. (2010) Superior Sphere ROI, coordinates: x=-27, y=-2, z=-17 millimetres [4]) and concentration of IN-OT (IN-[OT]) for Neutral emotions, divided by Group 1 (green), Group 2 (orange), and Group 3 or Control (blue).

However, it is important to emphasise that these observed changes in the intersecting lines do not reach statistical significance, as demonstrated by the results presented in Table 5.9.

The statistical analysis reveals that the main effects of [OT], Group, and Emotion all produce non-significant results with p-values exceeding the conventional threshold of 0.05. Specifically, the main effect of [OT] yields a corresponding p-value of 0.539, Group a p-value of 0.839 and Emotion presents a p-value of 0.719. Furthermore, the interaction effects among these variables also fail to attain statistical significance. The three-way interaction effect [OT] x Group x Emotion has a p-value of 0.569, [OT] x Group results in a p-value of 0.667, [OT] x Emotion yields a p-value of 0.691 and Group x Emotion a p-value of 0.644.

These non-significant p-values indicate that the observed changes in the intersecting lines do not reflect statistically meaningful relationships within the data.

Main Effects	**t-value**	**p-value**
[OT]	0.616	0.539
Group	0.175	0.839
Emotion	0.330	0.719
Interaction Effects	**F (Df)**	**p-value**
[OT] x Group x Emotion	0.880 (12)	0.569
[OT] x Group	0.801 (14)	0.667
[OT] x Emotion	0.779 (14)	0.691
Group x Emotion	0.814 (13)	0.644

Table 5.9: Statistical Results of the Interaction Effects of Intranasal Oxytocin (IN-[OT]), Group, and Emotion on Left Amygdala Activation (Gamer et al. (2010) Superior Sphere ROI, coordinates: x=-27, y=-2, z=-17 millimetres [4]) during the Facial Emotion Recognition Task. Abbreviations: Df, degrees of freedom.

5.3.2.3 Analysis of Gamer et al. (2010) Inferior Sphere ROI

Section 5.3.2.2 previously examined the coordinates of the superior left amygdala. In contrast, the focus of this section shifts towards the coordinates of the inferior left amygdala, as illustrated in Figure 5.6. It is important to note that during the process of subdividing and refining the analysed region, a reduction in the dataset occurred, resulting in the exclusion of additional subjects. Specifically, five levels of left amygdala activation were excluded from the analysis, leading to a reduced participant count of 52 for fearful emotions, 52 for happy emotions, and 50 for neutral emotions.

The provided graphs offer a visual representation of the relationship between IN-[OT] and left amygdala activation values across various groups. In Figure 5.22, the lines seem to follow a parallel trend, suggesting a lack of a significant interaction effect. In Figure 5.24, noteworthy interactions are observed between Group 2 and Control, as well as between Group 2 and Group 1, while the other groups do not display significant interactions. However, Figure 5.23 merits attention as it reveals a subtle but discernible degree of interaction among all the groups.

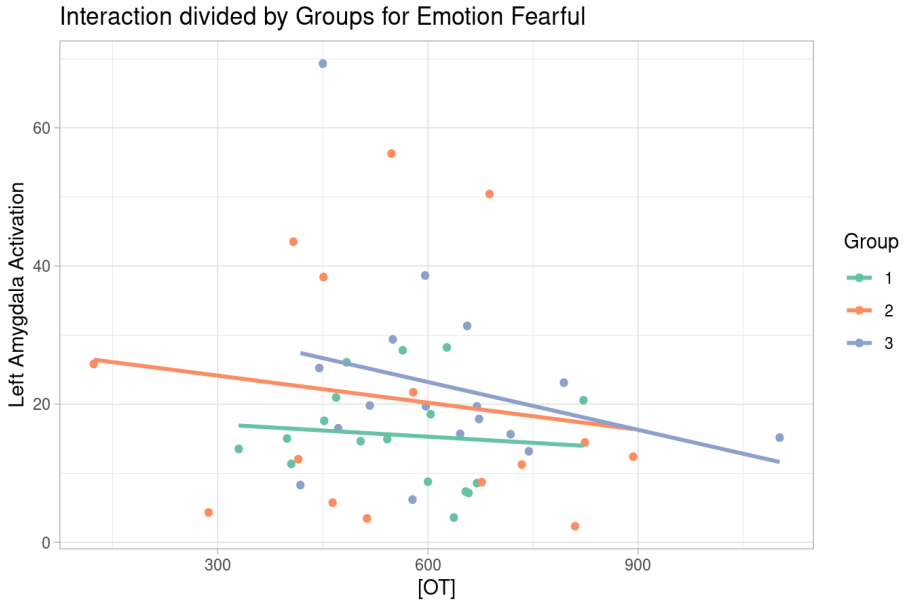

Figure 5.22: Scatterplot depicting the relationship between Left Amygdala Activation (Gamer et al. (2010) Inferior Sphere ROI, coordinates: x=-23, y=-3, z=-28 millimetres [4]) and concentration of IN-OT ([OT]) for Fearful emotions, divided by Group 1 (green), Group 2 (orange), and Group 3 or Control (blue).

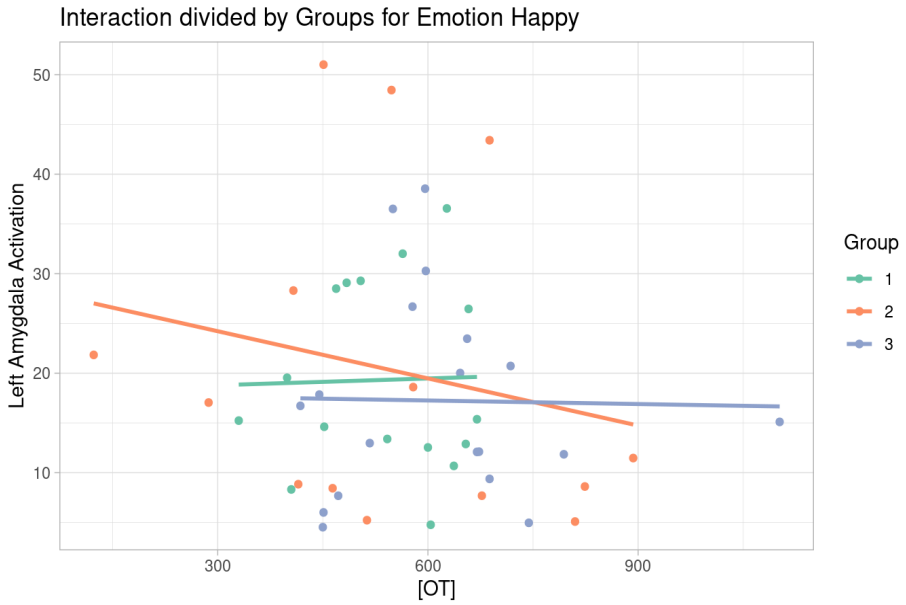

Figure 5.23: Scatterplot depicting the relationship between Left Amygdala Activation (Gamer et al. (2010) Inferior Sphere ROI, coordinates: x=-23, y=-3, z=-28 millimetres [4]) and concentration of IN-OT ([OT]) for Happy emotions, divided by Group 1 (green), Group 2 (orange), and Group 3 or Control (blue).

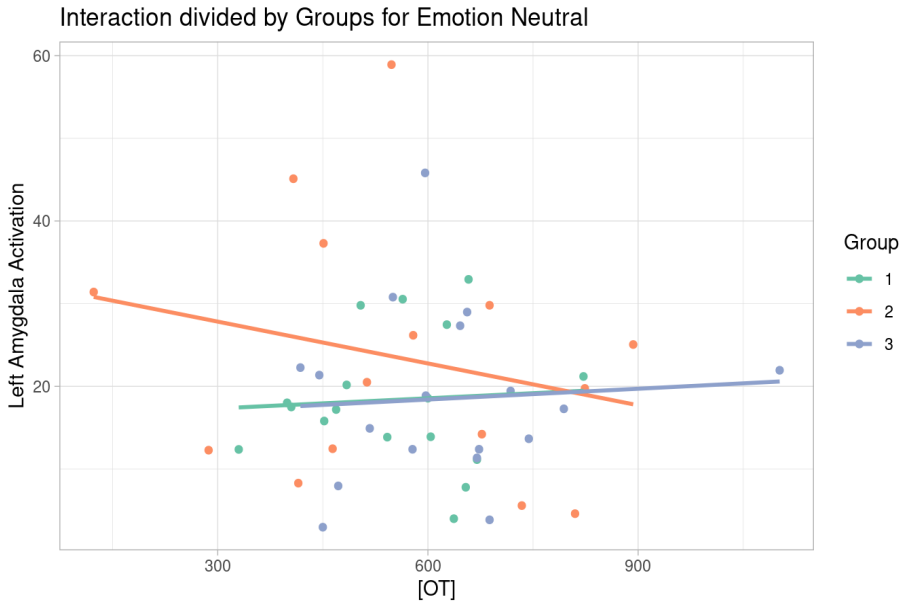

Figure 5.24: Scatterplot depicting the relationship between Left Amygdala Activation (Gamer et al. (2010) Inferior Sphere ROI, coordinates: x=-23, y=-3, z=-28 millimetres [4]) and concentration of IN-OT ([OT]) for Neutral emotions, divided by Group 1 (green), Group 2 (orange), and Group 3 or Control (blue).

Following an extensive statistical analysis, it has been ascertained that there is no statistically significant relationship evident among the considered variables. Referring to Table 5.10, it is noteworthy that all the main effects of the variables exceeded the threshold of 0.05, specifically registering at 0.930 for [OT], 0.313 for Group, and 0.925 for Emotion.

Similarly, the interaction effects produced p-values that approached 1.0, with the three-way interaction at 0.997, [OT] x Group at 0.999, [OT] x Emotion at 0.983, and Group x Emotion at 0.997. These p-values close to 1.0 underscore the limited evidence against the null hypothesis,

affirming the absence of statistically significant relationships between these variables.

Main Effects	**t-value**	**p-value**
[OT]	0.088	0.930
Group	1.171	0.313
Emotion	0.078	0.925
Interaction Effects	**F (Df)**	**p-value**
[OT] x Group x Emotion	0.225 (12)	0.997
[OT] x Group	0.204 (14)	0.999
[OT] x Emotion	0.361 (14)	0.983
Group x Emotion	0.248 (13)	0.997

Table 5.10: Statistical Results of the Interaction Effects of Intranasal Oxytocin (IN-[OT]), Group, and Emotion on Left Amygdala Activation (Gamer et al. (2010) Inferior Sphere ROI, coordinates: x=-23, y=-3, z=-28 millimetres [4]) during the Facial Emotion Recognition Task. Abbreviations: Df, degrees of freedom.

5.3.2.4 Analysis of AAL3 ROI

Next, the analysis of the AAL3 ROI was carried out, providing an anatomically precise representation of the left amygdala. In this analysis, no participant data was excluded, ensuring the inclusion of all 53 participants in the results.

In Figure 5.25 and 5.14, a parallel trend is evident between Group 2 and the Control group. This suggests that the outcomes for these two groups are moving in a similar direction or following a similar pattern. However, both of these groups exhibit a significant interaction with Group 1. In other words, Group 1 appears to play a distinctive role in affecting the relationship between these variables, even though Group 2 and the Control group show similar trends.

As for Figure 5.27, there is an interaction observed between Group 2 with both Group 1 and the Control group. This implies that when we examine the impact of Group 2 on the variables, it interacts significantly with both Group 1 and the Control group. Additionally, there is a subtle interaction observed between Group 1 and the Control group in this figure. This indicates that there is a mild, but still statistically significant, interaction between these two groups when considering the variables in question. This interaction may represent a nuanced influence that Group 1 has on the Control group's outcomes or responses related to the variables being studied.

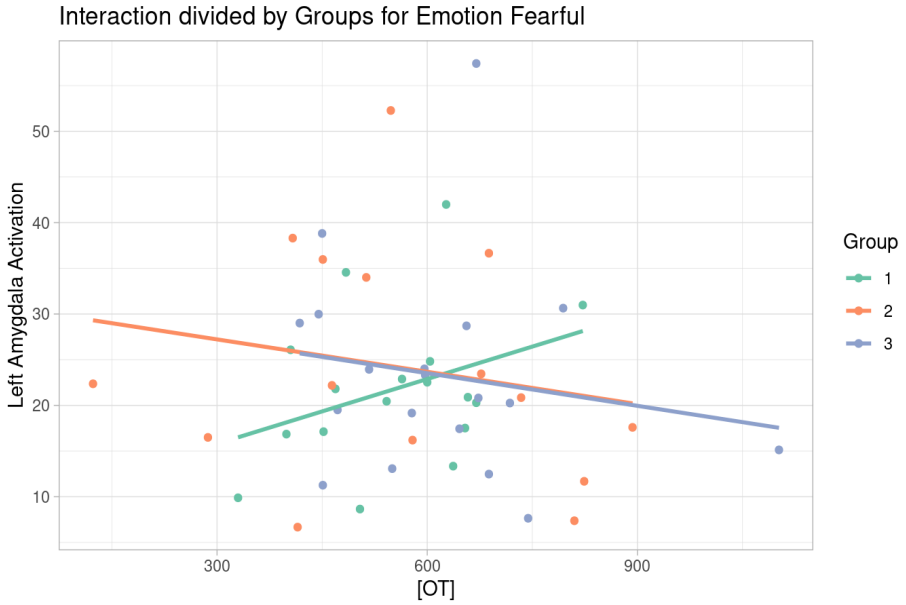

Figure 5.25: Scatterplot depicting the relationship between Left Amygdala Activation (AAL3 ROI, number: 45) and concentration of IN-OT ([OT]) for Fearful emotions, divided by Group 1 (green), Group 2 (orange), and Group 3 or Control (blue).

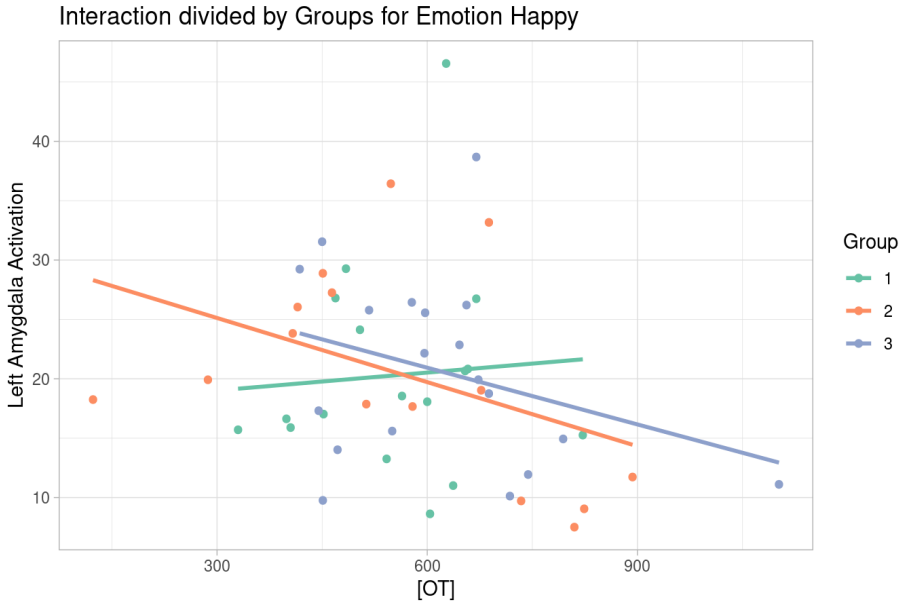

Figure 5.26: Scatterplot depicting the relationship between Left Amygdala Activation (AAL3 ROI, number: 45) and concentration of IN-OT ([OT]) for Happy emotions, divided by Group 1 (green), Group 2 (orange), and Group 3 or Control (blue).

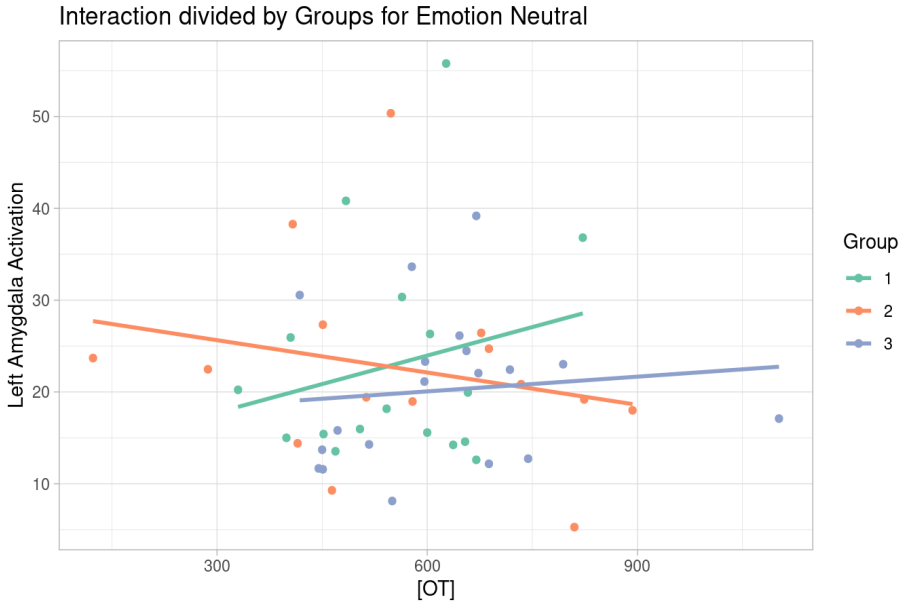

Figure 5.27: Scatterplot depicting the relationship between Left Amygdala Activation (AAL3 ROI, number: 45) and concentration of IN-OT ([OT]) for Neutral emotions, divided by Group 1 (green), Group 2 (orange), and Group 3 or Control (blue).

Nonetheless, in light of the results in Table 5.11, it becomes evident that none of the main effects or interaction effects achieved statistical significance, as all p-values substantially exceed the conventional significance level of 0.05. Consequently, these findings reinforce the notion that there is no statistically significant relationship or effect observed among the variables [OT], Group, Emotion, or their interactions.

In more specific terms, the main effects are as follows: [OT] has a p-value of 0.376, Group has a p-value of 0.983, and Emotion has a p-value of 0.597. Meanwhile, the interaction effects exhibit p-values of 0.939 for the three-way interaction, 0.950 for [OT] x Group, 0.976 for [OT] x Emotion, and a p-value of 0.952 for Group x Emotion.

Main Effects	**t-value**	**p-value**
[OT]	0.887	0.376
Group	0.017	0.983
Emotion	0.520	0.597
Interaction Effects	**F (Df)**	**p-value**
[OT] x Group x Emotion	0.451 (12)	0.939
[OT] x Group	0.461 (14)	0.950
[OT] x Emotion	0.389 (14)	0.976
Group x Emotion	0.440 (13)	0.952

Table 5.11: Statistical Results of the Interaction Effects of Intranasal Oxytocin (IN-[OT]), Group, and Emotion on Left Amygdala Activation (AAL3 ROI, number: 45) during the Facial Emotion Recognition Task. Abbreviations: Df, degrees of freedom.

In general, the results exposed throughout Section 3.2.1 and its subsections, show no significant interactions in any of the regions. As discussed in Section 3.2.2, a number of studies, including those by [40] and [71], have established a connection between OT and improved perfor-

mance in the face emotion recognition task among individuals with SCZ. In our study, occasional instances were noted where the graphs exhibited a greater resemblance between the SCZ-OT group and the control group, in line with our expectations (see Figures 5.20, 5.25, and 5.26). However, similar to several other studies [75–77], our research yielded mixed results.

This heterogeneity can be attributed to differences in dosing, frequency and administration protocols, the use of various clinical assessment tools and individual factors affecting oxytocin sensitivity [116]. For example in [40], 40 IU of IN-OT is employed alongside a block design. An interesting step to apply to our study is that, before drug administration and after the fMRI session, study participants from [40] were instructed to perform a visual analogue scale to examine mood changes that could confound the effects of oxytocin.

Moreover, it's important to note that inhaled OT may primarily have local effects via the olfactory nerve pathway leading to the brain, and its impact on global blood circulation may not be well-established. Therefore, we should avoid conflating blood sample concentration with the effects of inhaled OT. Specifically, it's worth mentioning that in a prior analysis in the study, when comparing OT concentration between pre and post OT administration, no significant differences were found across the whole study population. This suggests that there may have been no significant change in blood OT levels after OT administration.

Furthermore, [40] did not incorporate neutral faces as a control condition. This choice was influenced by prior research that has indicated abnormal amygdala responses to neutral faces in individuals with SCZ. Consequently, there is a need to identify a more suitable control condition that aligns with the objectives of our study. To overcome the potential issues with neutral faces researchers commonly opt for non-face control stimuli as a control condition. However, this approach carries the risk of blending activations associated with emotions and those tied to facial recognition processes [117].

Chapter 6

Conclusions and Future Work

This study was designed to examine the effects of IN-OT in patients with SCZ, during a face emotion recognition paradigm, which showed fearful, happy and neutral expressions. This investigation included a cohort of participants, comprising 17 patients with SCZ who received IN-OT, 18 patients with SCZ who received a PBO, and a control group consisting of 21 healthy individuals. It was hypothesised that patients who received OT exhibited amygdalar activation in the face emotion recognition task that closely resembled that of controls, as opposed to patients who had received PBO.

In the performance analysis, it was observed that patients with SCZ-PBO exhibited the longest reaction time and the lowest total rate of correct answers, along with the highest number of unanswered questions in comparison to SCZ-OT. This led to the inference that OT may have enhanced the performance of the patients. Nevertheless, from a statistical perspective, no significance was discerned, except for the case of a total good answer t-test between Group 1 and the control group, where statistical significance was indeed detected.

In the functional brain imaging analysis, activations in various brain regions known to be related to emotion recognition were detected, confirming their importance in social cognitive research. However, no activation of the amygdala was seen, and the two-sample T-test did not yield significant results, even with stringent significance criteria. This outcome suggests that methodological adjustments, such as reducing covariates and changing masking thresholds, should be considered. It is essential to recognise that these methodological changes may have an effect beyond the current analysis, potentially influencing our region of interest examination in the region of interest.

In the analysis of the region of interest performed for IN-OT in various ROI, graphical interactions between groups were identified, occasionally revealing a greater resemblance between SCZ-OT and the control group, as anticipated (Figures 5.20, 5.25 and 5.26). Nonetheless, it is noteworthy that statistical significance was not detected in any of the distinct regions.

An additional analysis was carried out with respect to the endogenous OT values, motivated by previous studies that had associated elevated levels of endogenous OT with improved facial recognition, as mentioned in Section 3.2.1. In the course of this analysis, graphical interactions between groups were discerned, occasionally indicating a greater degree of similarity between SCZ-OT and the control group (Figures 5.3, 5.8 and 5.12). However, it is important to note that no statistical significance was observed in any of the distinct regions.

Studies on amygdala activation often fail to replicate earlier results or show no significant findings [117]. Variations in lateralisation have been observed, with one study suggesting a right

laterality bias due to the visuospatial processing demands of their paradigm [118]. Reproducibility studies have indicated that amygdala activation is the least reproducible, both at the group and single-subject levels and that reproducibility decreases after correcting for physiological noise [119]. Amygdala activations in response to emotional stimuli can be triggered through a variety of methods, including auditory, haptic, and intrinsic stimuli [120].

In conclusion, these findings emphasise the intricate interplay between methodological decisions and research outcomes in the field of neuroimaging, highlighting the significance of thorough deliberation and continued exploration to advance our understanding of emotion processing in the human brain. It is crucial to acknowledge specific methodological considerations that may have influenced our results.

Firstly, the initial model used had a limited number of trials available for estimating each regression due to the division of trials by sex and screen position. With only 6 trials available for each regression, this may have posed limitations, especially if sex type and position were not extensively used in the analysis. In retrospect, a model without those would allow for a more robust estimation.

Secondly, considering that some participants with SCZ exhibited a low rate of response, it would have been beneficial to implement more extensive controls, such as debriefing procedures or additional subject training before the scanning session. These measures could potentially enhance the reliability of participant responses and minimise variability in the data.

Lastly, it is important to note that our study involved small populations in each group. While this is not uncommon when working with patients, it does introduce some statistical limitations. However, it is worth mentioning that conducting research with patient populations, particularly those with conditions like SCZ, can be inherently challenging due to factors such as recruitment and compliance. Despite these challenges, the insights gained from this study contribute to our broader understanding of emotion processing in clinical contexts.

Appendix A

One-Sample T-test

Fearful				
	Peak MNI Coordinates			
T-value	**x (mm)**	**y (mm)**	**z (mm)**	**Cluster Labelling**
9.43	**36**	**-64**	**-18**	Fusiform_R
8.04	-40	-78	-18	Fusiform_L
Happy				
	Peak MNI Coordinates			
T-value	**x (mm)**	**y (mm)**	**z (mm)**	**Cluster Labelling**
9.94	38	-64	-22	Cerebelum_6_R
77.71	**38**	**-46**	**-28**	Temporal_Inf_R
Neutral				
	Peak MNI Coordinates			
T-value	**x (mm)**	**y (mm)**	**z (mm)**	**Cluster Labelling**
9.79	**38**	**-60**	**-22**	Cerebelum_6_R
8.76	-42	-48	-28	Cerebelum_Crus1_L

Table A.1: Significant regions at p<0.05 FWE corrected, for the effect of the different emotions during Face Emotion Recognition Task on Group 2. The coordinates in bold represent the nearest local maximum represented in Figure A.1. Abbreviations (from AAL3): Fusiform_R, right fusiform; Fusiform_L, left fusiform; Cerebelum_6_R, right lobule VI of cerebellar hemisphere; Temporal_Inf_R, right inferior temporal gyrus; Cerebelum_Crus1_L, left crus I of the cerebellar hemisphere.

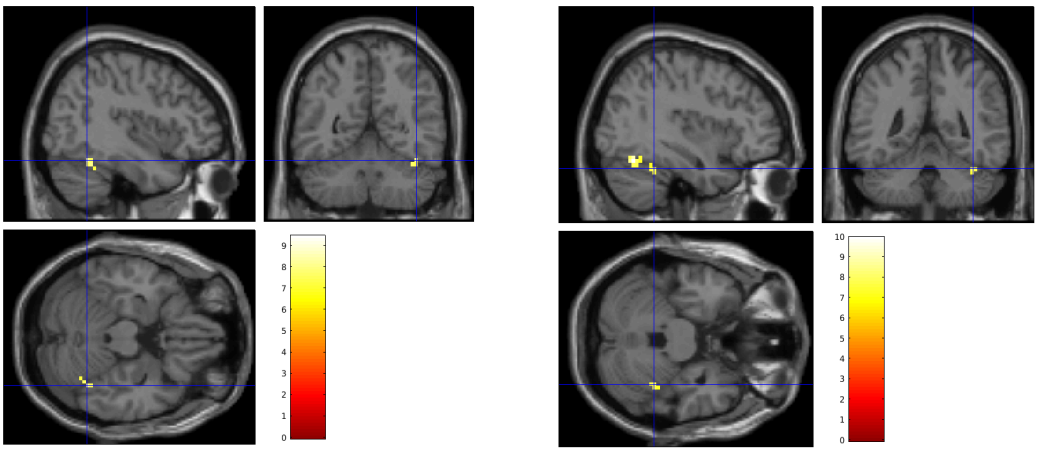

(a)

(b)

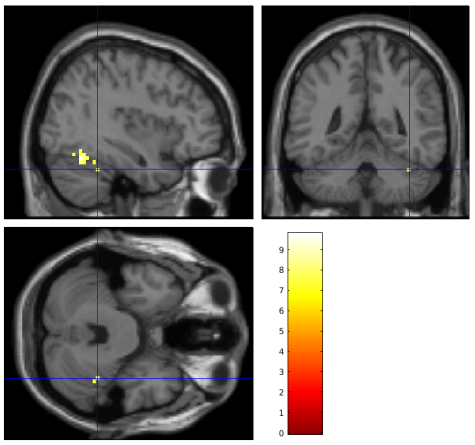

(c)

Figure A.1: Sagittal, Axial, and Coronal Slices of the significant regions at p<0.05 FWE corrected for the positive effect on the Fearful, Happy and Neutral contrast in Group 2 during the Face Emotion Recognition Task. There is little to no activation in all regions (colour bars indicate T-values). The blue cross represents the nearest local maximum with its coordinates in bold in Table A.1. (a) Activation for Fearful contrast (p=0.010, 0 cluster, corrected), displayed on an anatomical slice (x=36, y=-64, z=-18) in the right fusiform. (b) Activation of Happy contrast (p=0.015, 0 cluster, corrected), displayed on an anatomical slice (x=38, y=-46, z=-28) in the right inferior temporal gyrus. (c) Activation for Neutral contrast (p=0.001, 0 cluster, corrected), displayed on an anatomical slice (x=38, y=-60, z=-22) in the right lobule VI of the cerebellar hemisphere.

Fearful				
	Peak MNI Coordinates			
T-value	**x (mm)**	**y (mm)**	**z (mm)**	**Cluster Labelling**
8.83	**42**	**-54**	**-24**	Cerebelum_6_R
7.42	-42	-66	-18	Fusiform_L
Happy				
	Peak MNI Coordinates			
T-value	**x (mm)**	**y (mm)**	**z (mm)**	**Cluster Labelling**
8.89	-36	-58	-24	Cerebelum_6_L
7.94	42	-58	-28	Cerebelum_Crus1_R
7.47	-40	-58	-34	Cerebelum_Crus1_L
7.08	36	-70	-22	Cerebelum_6_R
6.78	-36	-70	-18	Cerebelum_6_L
6.75	42	-76	-12	Occipital_Inf_R
6.71	44	-84	-4	Occipital_Inf_R
6.68	48	-76	-10	Occipital_Inf_R
6.67	**36**	**-42**	**-28**	Cerebelum_6_R
6.63	-36	-70	-12	Fusiform_L
Neutral				
	Peak MNI Coordinates			
T-value	**x (mm)**	**y (mm)**	**z (mm)**	**Cluster Labelling**
7.25	38	-48	-24	Cerebelum_6_R
7.22	-36	-54	-22	Cerebelum_6_L
7.12	-42	-70	-16	Fusiform_L
6.92	-6	2	42	Cingulum_Mid_L
6.88	42	-54	-24	Cerebelum_6_R
6.87	**-4**	**-4**	**48**	Cingulum_Mid_L

Table A.2: Significant regions at $p<0.05$ FWE corrected, for the effect of the different emotions during Face Emotion Recognition Task on Control. The coordinates in bold represent the nearest local maximum represented in Figure A.2. Abbreviations (from AAL3): Cerebelum_6_R, right lobule VI of cerebellar hemisphere; Fusiform_L, left fusiform; Cerebelum_6_L, left lobule VI of cerebellar hemisphere; Cerebelum_Crus1_R, right crus I of the cerebellar hemisphere; Cerebelum_Crus1_L, left crus I of the cerebellar hemisphere; Occipital_Inf_R, right inferior occipital gyrus; Cingulum_Mid_L, left median cingulate and paracingulate gyri.

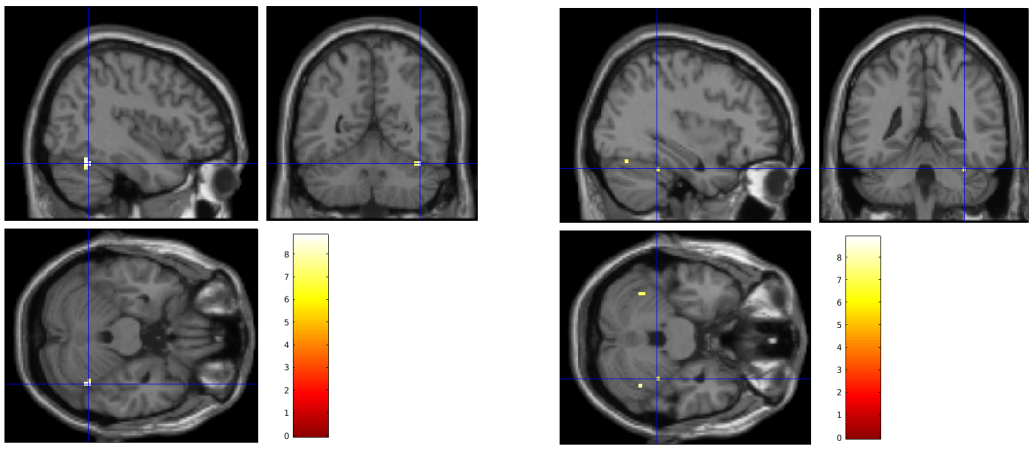

(a) (b)

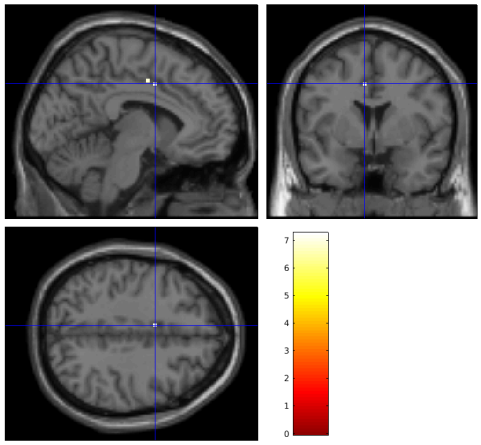

(c)

Figure A.2: Sagittal, Axial, and Coronal Slices of the significant regions at p<0.05 FWE corrected for the positive effect on the Fearful, Happy and Neutral contrast in Control group during the Face Emotion Recognition Task. There is little to no activation in all regions (colour bars indicate T-values). The blue cross represents the nearest local maximum with its coordinates in bold in Table A.2. (a) Activation for Fearful contrast (p=0.001, 0 cluster, corrected), displayed on an anatomical slice (x=42, y=-54, z=-24) in the right lobule VI of cerebellar hemisphere. (b) Activation of Happy contrast (p=0.045, 0 cluster, corrected), displayed on an anatomical slice (x=36, y=-42, z=-28) in the right lobule VI of cerebellar hemisphere. (c) Activation for Neutral contrast (p=0.026, 0 cluster, corrected), displayed on an anatomical slice (x=-4, y=-4, z=48) in the left median cingulate and paracingulate gyri.

References

[1] S. G. Costafreda, M. J. Brammer, A. S. David, and C. H. Fu, "Predictors of amygdala activation during the processing of emotional stimuli: A meta-analysis of 385 PET and fMRI studies," *Brain Research Reviews*, vol. 58, pp. 57–70, June 2008.

[2] H.-J. Lee, A. H. Macbeth, J. Pagani, and W. S. Young, "Oxytocin: The great facilitator of life," *Progress in Neurobiology*, Apr. 2009.

[3] M. A. Lindquist, J. M. Loh, L. Y. Atlas, and T. D. Wager, "Modeling the hemodynamic response function in fMRI: Efficiency, bias and mis-modeling," *NeuroImage*, vol. 45, pp. S187–S198, Mar. 2009.

[4] M. Gamer, B. Zurowski, and C. Büchel, "Different amygdala subregions mediate valence-related and attentional effects of oxytocin in humans," *Proceedings of the National Academy of Sciences*, vol. 107, pp. 9400–9405, Apr. 2010.

[5] J. G. Pouget and D. J. Müller, "Pharmacogenetics of antipsychotic treatment in schizophrenia," in *Methods in Molecular Biology*, pp. 557–587, Springer New York, 2014.

[6] K. K. Goh, C.-H. Chen, and H.-Y. Lane, "Oxytocin in schizophrenia: Pathophysiology and implications for future treatment," *International Journal of Molecular Sciences*, vol. 22, p. 2146, Feb. 2021.

[7] P. D. Shilling and D. Feifel, "Potential of oxytocin in the treatment of schizophrenia," *CNS Drugs*, vol. 30, pp. 193–208, Feb. 2016.

[8] M. F. Green, D. L. Penn, R. Bentall, W. T. Carpenter, W. Gaebel, R. C. Gur, A. M. Kring, S. Park, S. M. Silverstein, and R. Heinssen, "Social cognition in schizophrenia: An NIMH workshop on definitions, assessment, and research opportunities," *Schizophrenia Bulletin*, vol. 34, pp. 1211–1220, Aug. 2008.

[9] A. J. Guastella, P. B. Ward, I. B. Hickie, S. Shahrestani, M. A. R. Hodge, E. M. Scott, and R. Langdon, "A single dose of oxytocin nasal spray improves higher-order social cognition in schizophrenia," *Schizophrenia Research*, vol. 168, pp. 628–633, Nov. 2015.

[10] L. F. Jarskog, C. A. Pedersen, J. L. Johnson, R. M. Hamer, S. W. Rau, T. Elliott, and D. L. Penn, "A 12-week randomized controlled trial of twice-daily intranasal oxytocin for social cognitive deficits in people with schizophrenia," *Schizophrenia Research*, vol. 185, pp. 88–95, July 2017.

[11] T. T. Yang, V. Menon, S. Eliez, C. Blasey, C. D. White, A. J. Reid, I. H. Gotlib, and A. L. Reiss, "Amygdalar activation associated with positive and negative facial expressions," *NeuroReport*, vol. 13, pp. 1737–1741, Oct. 2002.

[12] M. Arioli, C. Crespi, and N. Canessa, "Social cognition through the lens of cognitive and clinical neuroscience," *BioMed Research International*, vol. 2018, pp. 1–18, Sept. 2018.

[13] R. Ivell and D. Richter, "Structure and comparison of the oxytocin and vasopressin genes from rat.," *Proceedings of the National Academy of Sciences*, vol. 81, pp. 2006–2010, Apr. 1984.

[14] A. Romano, B. Tempesta, M. V. M. D. Bonaventura, and S. Gaetani, "From autism to eating disorders and more: The role of oxytocin in neuropsychiatric disorders," *Frontiers in Neuroscience*, vol. 9, Jan. 2016.

[15] A. Doruyter, N. A. Groenewold, P. Dupont, D. J. Stein, and J. M. Warwick, "Resting-state fMRI and social cognition: An opportunity to connect," *Human Psychopharmacology: Clinical and Experimental*, vol. 32, p. e2627, Aug. 2017.

[16] N. K. Logothetis, J. Pauls, M. Augath, T. Trinath, and A. Oeltermann, "Neurophysiological investigation of the basis of the fMRI signal," *Nature*, vol. 412, pp. 150–157, July 2001.

[17] D. A. Leopold and G. Rhodes, "A comparative view of face perception.," *Journal of Comparative Psychology*, vol. 124, no. 3, pp. 233–251, 2010.

[18] B. Montagne, R. P. C. Kessels, E. H. F. D. Haan, and D. I. Perrett, "The emotion recognition task: A paradigm to measure the perception of facial emotional expressions at different intensities," *Perceptual and Motor Skills*, vol. 104, pp. 589–598, Apr. 2007.

[19] V. Ferretti and F. Papaleo, "Understanding others: emotion recognition abilities in humans and other animals," *Genes, Brain and Behavior*, p. e12544, Dec. 2018.

[20] D. Bzdok, A. R. Laird, K. Zilles, P. T. Fox, and S. B. Eickhoff, "An investigation of the structural, connectional, and functional subspecialization in the human amygdala," *Human Brain Mapping*, vol. 34, pp. 3247–3266, July 2012.

[21] M. Pabba, "Evolutionary development of the amygdaloid complex," *Frontiers in Neuroanatomy*, vol. 7, 2013.

[22] G. Šimić, M. Tkalčić, V. Vukić, D. Mulc, E. Španić, M. Šagud, F. E. Olucha-Bordonau, M. Vukšić, and P. R. Hof, "Understanding emotions: Origins and roles of the amygdala," *Biomolecules*, vol. 11, p. 823, May 2021.

[23] D. Keltner, P. Ekman, G. C. Gonzaga, and J. Beer, "Facial expression of emotion," in *Handbook of affective sciences* (R. J. Davidson, K. R. Scherer, and H. H. Goldsmith, eds.), pp. 415–432, Oxford University Press, 2003.

[24] S. F. Taylor, J. Kang, I. S. Brege, I. F. Tso, A. Hosanagar, and T. D. Johnson, "Meta-analysis of functional neuroimaging studies of emotion perception and experience in schizophrenia," *Biological Psychiatry*, vol. 71, pp. 136–145, Jan. 2012.

[25] A. Millier, U. Schmidt, M. Angermeyer, D. Chauhan, V. Murthy, M. Toumi, and N. Cadi-Soussi, "Humanistic burden in schizophrenia: A literature review," *Journal of Psychiatric Research*, vol. 54, pp. 85–93, July 2014.

[26] *Diagnostic and Statistical Manual of Mental Disorders*. American Psychiatric Association, 2013.

[27] D. I. Driver, S. Thomas, N. Gogtay, and J. L. Rapoport, "Childhood-onset schizophrenia and early-onset schizophrenia spectrum disorders," *Child and Adolescent Psychiatric Clinics of North America*, vol. 29, pp. 71–90, Jan. 2020.

[28] H. Häfner, K. Maurer, W. Löffler, B. Fätkenheuer, W. an der Heiden, A. Riecher-Rössler, S. Behrens, and W. F. Gattaz, "The epidemiology of early schizophrenia. Influence of age and gender on onset and early course," *The British Journal of Psychiatry. Supplement*, pp. 29–38, Apr. 1994.

[29] E. J. Nestler, P. J. Kenny, S. J. Russo, and A. Schafer, *Molecular neuropharmacology: A foundation for clinical neuroscience*. McGraw Hill, 2020.

[30] A. Cavieres, V. Acuña, M. Arancibia, and N. Lopetegui, "Differences in social perception in people with schizophrenia and bipolar disorder," *Schizophrenia Research: Cognition*, vol. 33, p. 100286, Sept. 2023.

[31] G. M. B. Kitoko, P. Maurage, S. M. ma Miezi, B. Gillain, A. P. Kiswanga, and E. Constant, "Inter-individual variability of social perception and social knowledge impairments among patients with schizophrenia," *Psychiatry Research*, vol. 290, p. 112951, Aug. 2020.

[32] T. M. Karpouzian, E. C. Alden, J. L. Reilly, and M. J. Smith, "High functioning individuals with schizophrenia have preserved social perception but not mentalizing abilities," *Schizophrenia Research*, vol. 171, pp. 137–139, Mar. 2016.

[33] J. Lee, R. S. Kern, P.-O. Harvey, W. P. Horan, K. S. Kee, K. Ochsner, D. L. Penn, and M. F. Green, "An intact social cognitive process in schizophrenia: Situational context effects on perception of facial affect," *Schizophrenia Bulletin*, vol. 39, pp. 640–647, Apr. 2012.

[34] H. H. Dale, "On some physiological actions of ergot," *The Journal of Physiology*, vol. 34, pp. 163–206, May 1906.

[35] W. S. Young and H. Gainer, "Transgenesis and the study of expression, cellular targeting and function of oxytocin, vasopressin and their receptors," *Neuroendocrinology*, vol. 78, no. 4, pp. 185–203, 2003.

[36] A. Meyer-Lindenberg, G. Domes, P. Kirsch, and M. Heinrichs, "Oxytocin and vasopressin in the human brain: social neuropeptides for translational medicine," *Nature Reviews Neuroscience*, vol. 12, pp. 524–538, Aug. 2011.

[37] H. Beckmann, R. E. Lang, and W. F. Gattaz, "Vasopressin-oxytocin in cerebrospinal fluid of schizophrenic patients and normal controls," *Psychoneuroendocrinology*, vol. 10, pp. 187–191, Jan. 1985.

[38] D. Glovinsky, K. Kalogeras, D. Kirch, R. Suddath, and R. Wyatt, "Cerebrospinal fluid oxytocin concentration in schizophrenic patients does not differ from control subjects and is not changed by neuroleptic medication," *Schizophrenia Research*, vol. 11, pp. 273–276, Feb. 1994.

[39] D. Feifel and T. Reza, "Oxytocin modulates psychotomimetic-induced deficits in sensorimotor gating," *Psychopharmacology*, vol. 141, pp. 93–98, Jan. 1999.

[40] N. Y. Shin, H. Y. Park, W. H. Jung, J. W. Park, J.-Y. Yun, J. H. Jang, S. N. Kim, H. J. Han, S.-Y. Kim, D.-H. Kang, and J. S. Kwon, "Effects of oxytocin on neural response to facial expressions in patients with schizophrenia," *Neuropsychopharmacology*, vol. 40, pp. 1919–1927, Feb. 2015.

[41] A. Webb, *Introduction to biomedical imaging*. Wiley, 2003.

[42] J. C. Gore, "Principles and practice of functional MRI of the human brain," *Journal of Clinical Investigation*, vol. 112, pp. 4–9, July 2003.

[43] M. A. Brown and R. C. Semelka, *MRI: Basic principles and applications*. John Wiley amp; Sons, Inc., 2011.

[44] B. N. Smith and A. G. Webb, *Introduction to medical imaging: Physics, engineering and clinical applications*. Cambridge University Press, 2012.

[45] J. G. Webster, *Medical instrumentation: Application and design*. 2009.

[46] L. Pauling and C. D. Coryell, "The magnetic properties and structure of hemoglobin, oxyhemoglobin and carbonmonoxyhemoglobin," *Proceedings of the National Academy of Sciences*, vol. 22, pp. 210–216, Apr. 1936.

[47] P. T. Fox, M. E. Raichle, M. A. Mintun, and C. Dence, "Nonoxidative glucose consumption during focal physiologic neural activity," *Science*, vol. 241, pp. 462–464, July 1988.

[48] K. R. Thulborn, J. C. Waterton, P. M. Matthews, and G. K. Radda, "Oxygenation dependence of the transverse relaxation time of water protons in whole blood at high field," *Biochimica et Biophysica Acta (BBA) - General Subjects*, vol. 714, pp. 265–270, Feb. 1982.

[49] S. Ogawa, T. M. Lee, A. R. Kay, and D. W. Tank, "Brain magnetic resonance imaging with contrast dependent on blood oxygenation.," *Proceedings of the National Academy of Sciences*, vol. 87, pp. 9868–9872, Dec. 1990.

[50] R. B. Buxton, "The elusive initial dip," *NeuroImage*, vol. 13, pp. 953–958, June 2001.

[51] K. Friston, P. Fletcher, O. Josephs, A. Holmes, M. Rugg, and R. Turner, "Event-related fMRI: Characterizing differential responses," *NeuroImage*, vol. 7, pp. 30–40, Jan. 1998.

[52] K. J. Friston, A. P. Holmes, K. J. Worsley, J.-P. Poline, C. D. Frith, and R. S. J. Frackowiak, "Statistical parametric maps in functional imaging: A general linear approach," *Human Brain Mapping*, vol. 2, no. 4, pp. 189–210, 1994.

[53] K. J. Friston, C. D. Frith, P. F. Liddle, and R. S. J. Frackowiak, "Comparing functional (PET) images: The assessment of significant change," *Journal of Cerebral Blood Flow &amp Metabolism*, vol. 11, pp. 690–699, July 1991.

[54] K. J. Friston, "Models of brain function in neuroimaging," *Annual Review of Psychology*, vol. 56, pp. 57–87, Feb. 2005.

[55] C. F. Zink and A. Meyer-Lindenberg, "Human neuroimaging of oxytocin and vasopressin in social cognition," *Hormones and Behavior*, vol. 61, pp. 400–409, Mar. 2012.

[56] R. Adolphs, "What does the amygdala contribute to social cognition?," *Annals of the New York Academy of Sciences*, vol. 1191, pp. 42–61, Mar. 2010.

[57] D. Huber, P. Veinante, and R. Stoop, "Vasopressin and oxytocin excite distinct neuronal populations in the central amygdala," *Science*, vol. 308, pp. 245–248, Apr. 2005.

[58] J. N. Ferguson, J. M. Aldag, T. R. Insel, and L. J. Young, "Oxytocin in the medial amygdala is essential for social recognition in the mouse," *The Journal of Neuroscience*, vol. 21, pp. 8278–8285, Oct. 2001.

[59] P. Kirsch, C. Esslinger, Q. Chen, D. Mier, S. Lis, S. Siddhanti, H. Gruppe, V. S. Mattay, B. Gallhofer, and A. Meyer-Lindenberg, "Oxytocin modulates neural circuitry for social cognition and fear in humans," *The Journal of Neuroscience*, vol. 25, pp. 11489–11493, Dec. 2005.

[60] G. Domes, M. Heinrichs, J. Gläscher, C. Büchel, D. F. Braus, and S. C. Herpertz, "Oxytocin attenuates amygdala responses to emotional faces regardless of valence," *Biological Psychiatry*, vol. 62, pp. 1187–1190, Nov. 2007.

[61] P. Petrovic, R. Kalisch, T. Singer, and R. J. Dolan, "Oxytocin attenuates affective evaluations of conditioned faces and amygdala activity," *Journal of Neuroscience*, vol. 28, pp. 6607–6615, June 2008.

[62] M. Heinrichs, B. von Dawans, and G. Domes, "Oxytocin, vasopressin, and human social behavior," *Frontiers in Neuroendocrinology*, vol. 30, pp. 548–557, Oct. 2009.

[63] G. P. Strauss, W. R. Keller, J. I. Koenig, J. M. Gold, K. L. Ossenfort, and R. W. Buchanan, "Plasma oxytocin levels predict olfactory identification and negative symptoms in individuals with schizophrenia," *Schizophrenia Research*, vol. 162, pp. 57–61, Mar. 2015.

[64] G. P. Strauss, W. R. Keller, J. I. Koenig, S. K. Sullivan, J. M. Gold, and R. W. Buchanan, "Endogenous oxytocin levels are associated with the perception of emotion in dynamic body expressions in schizophrenia," *Schizophrenia Research*, vol. 162, pp. 52–56, Mar. 2015.

[65] L. H. Rubin, C. S. Carter, J. R. Bishop, H. Pournajafi-Nazarloo, M. S. Harris, S. K. Hill, J. L. Reilly, and J. A. Sweeney, "Peripheral vasopressin but not oxytocin relates to severity of acute psychosis in women with acutely-ill untreated first-episode psychosis," *Schizophrenia Research*, vol. 146, pp. 138–143, May 2013.

[66] K. Balikci, O. Aydin, C. Tas, and A. E. Danaci, "Oxytocin and social cognition in patients with schizophrenia: comparison with healthy siblings and healthy controls," *Psychiatry and Clinical Psychopharmacology*, vol. 28, pp. 123–130, Oct. 2017.

[67] O. Aydın, P. H. Lysaker, K. Balıkçı, P. Ünal Aydın, and A. Esen-Danacı, "Associations of oxytocin and vasopressin plasma levels with neurocognitive, social cognitive and meta cognitive function in schizophrenia," *Psychiatry Research*, vol. 270, pp. 1010–1016, Dec. 2018.

[68] G. P. Strauss, H. C. Chapman, W. R. Keller, J. I. Koenig, J. M. Gold, W. T. Carpenter, and R. W. Buchanan, "Endogenous oxytocin levels are associated with impaired social cognition and neurocognition in schizophrenia," *Journal of Psychiatric Research*, vol. 112, pp. 38–43, May 2019.

[69] K. Frost, W. Keller, R. Buchanan, J. Gold, J. Koenig, K. Ossenfort, A. Katz, and G. Strauss, "C-14* plasma oxytocin levels are associated with impaired social cognition and neurocognition in schizophrenia," *Archives of Clinical Neuropsychology*, vol. 29, pp. 577–578, Aug. 2014.

[70] B. B. Averbeck, T. Bobin, S. Evans, and S. S. Shergill, "Emotion recognition and oxytocin in patients with schizophrenia," *Psychological Medicine*, vol. 42, pp. 259–266, Aug. 2011.

[71] C. M. Gibson, D. L. Penn, K. L. Smedley, J. Leserman, T. Elliott, and C. A. Pedersen, "A pilot six-week randomized controlled trial of oxytocin on social cognition and social skills in schizophrenia," *Schizophrenia Research*, vol. 156, pp. 261–265, July 2014.

[72] M. B. Goldman, A. M. Gomes, C. S. Carter, and R. Lee, "Divergent effects of two different doses of intranasal oxytocin on facial affect discrimination in schizophrenic patients with and without polydipsia," *Psychopharmacology*, vol. 216, pp. 101–110, Feb. 2011.

[73] M. C. Davis, J. Lee, W. P. Horan, A. D. Clarke, M. R. McGee, M. F. Green, and S. R. Marder, "Effects of single dose intranasal oxytocin on social cognition in schizophrenia," *Schizophrenia Research*, vol. 147, pp. 393–397, July 2013.

[74] D. Feifel, K. Macdonald, A. Nguyen, P. Cobb, H. Warlan, B. Galangue, A. Minassian, O. Becker, J. Cooper, W. Perry, M. Lefebvre, J. Gonzales, and A. Hadley, "Adjunctive intranasal oxytocin reduces symptoms in schizophrenia patients," *Biological Psychiatry*, vol. 68, pp. 678–680, Oct. 2010.

[75] C. Cacciotti-Saija, R. Langdon, P. B. Ward, I. B. Hickie, E. M. Scott, S. L. Naismith, L. Moore, G. A. Alvares, M. A. R. Hodge, and A. J. Guastella, "A double-blind randomized controlled trial of oxytocin nasal spray and social cognition training for young people with early psychosis," *Schizophrenia Bulletin*, vol. 41, pp. 483–493, June 2014.

[76] L. R. H. de Macedo, A. W. Zuardi, J. P. M. de Sousa, M. H. N. Chagas, and J. E. Hallak, "Oxytocin does not improve performance of patients with schizophrenia and healthy volunteers in a facial emotion matching task," *Psychiatry Research*, vol. 220, pp. 125–128, Dec. 2014.

[77] G. P. Strauss, E. Granholm, J. L. Holden, I. Ruiz, J. M. Gold, D. L. Kelly, and R. W. Buchanan, "The effects of combined oxytocin and cognitive behavioral social skills training on social cognition in schizophrenia," *Psychological Medicine*, vol. 49, pp. 1731–1739, Sept. 2018.

[78] H. C. Santos, A. Rodrigues, S. Ferreira, J. M. Martins, T. Baptista, J. G. Marques, B. Kirkpatrick, and D. Prata, "The european portuguese version of the brief negative symptom scale," *Psychopathology*, pp. 1–1, June 2023.

[79] M. Heinrichs and G. Domes, "Neuropeptides and social behaviour: Effects of oxytocin and vasopressin in humans," *Progress in Brain Research*, p. 337–350, 2008.

[80] G. Cosme, P. Arriaga, P. J. Rosa, M. A. Mehta, and D. Prata, "Temporal profile of intranasal oxytocin in the human autonomic nervous system at rest: An electrocardiography and pupillometry study," *Journal of Psychopharmacology*, vol. 37, pp. 566–576, Mar. 2023.

[81] "Statistical parametric mapping." `http://www.fil.ion.ucl.ac.uk/spm`. Accessed: September 15, 2022.

[82] *Statistical Parametric Mapping: The Analysis of Functional Brain Images*. Elsevier, 2007.

[83] S. Ulmer and O. Jansen, *FMRI: Basics and clinical applications*. Springer, 2020.

[84] A. Collignon, F. Maes, D. Delaere, D. Vandermeulen, P. Suetens, and G. Marchal, "Automated multi-modality image registration based on information theory," *Information Processing in Medical Imaging*, vol. 3, no. 6, pp. 263–274, 1995.

[85] J. Ashburner, "Computational anatomy with the SPM software," *Magnetic Resonance Imaging*, vol. 27, pp. 1163–1174, Oct. 2009.

[86] O. Esteban *et al.*, "Fmriprep: A robust preprocessing pipeline for functional mri," *Nature Methods*, vol. 16, no. 1, p. 111–116, 2018.

[87] O. Esteban, C. J. Markiewicz, M. Goncalves, C. Provins, J. D. Kent, E. DuPre, T. Salo, R. Ciric, B. Pinsard, R. W. Blair, R. A. Poldrack, and K. J. Gorgolewski, "fmriprep: a robust preprocessing pipeline for functional mri," 2023.

[88] K. Gorgolewski, C. D. Burns, C. Madison, D. Clark, Y. O. Halchenko, M. L. Waskom, and S. S. Ghosh, "Nipype: A flexible, lightweight and extensible neuroimaging data processing framework in python," *Frontiers in Neuroinformatics*, vol. 5, 2011.

[89] O. Esteban *et al.*, "nipy/nipype: 1.8.3," 2022.

[90] B. Avants, C. Epstein, M. Grossman, and J. Gee, "Symmetric diffeomorphic image registration with cross-correlation: Evaluating automated labeling of elderly and neurodegenerative brain," *Medical Image Analysis*, vol. 12, no. 1, p. 26–41, 2008.

[91] Y. Zhang, M. Brady, and S. Smith, "Segmentation of brain MR images through a hidden markov random field model and the expectation-maximization algorithm," *IEEE Transactions on Medical Imaging*, vol. 20, no. 1, pp. 45–57, 2001.

[92] A. M. Dale, B. Fischl, and M. I. Sereno, "Cortical surface-based analysis," *NeuroImage*, vol. 9, pp. 179–194, Feb. 1999.

[93] A. Klein, S. S. Ghosh, F. S. Bao, J. Giard, Y. Häme, E. Stavsky, N. Lee, B. Rossa, M. Reuter, E. C. Neto, and A. Keshavan, "Mindboggling morphometry of human brains," *PLOS Computational Biology*, vol. 13, p. e1005350, Feb. 2017.

[94] V. Fonov, A. Evans, R. McKinstry, C. Almli, and D. Collins, "Unbiased nonlinear average age-appropriate brain templates from birth to adulthood," *NeuroImage*, vol. 47, p. S102, July 2009.

[95] M. F. Glasser, S. N. Sotiropoulos, J. A. Wilson, T. S. Coalson, B. Fischl, J. L. Andersson, J. Xu, S. Jbabdi, M. Webster, J. R. Polimeni, D. C. V. Essen, and M. Jenkinson, "The minimal preprocessing pipelines for the human connectome project," *NeuroImage*, vol. 80, pp. 105–124, Oct. 2013.

[96] M. Jenkinson, P. Bannister, M. Brady, and S. Smith, "Improved optimization for the robust and accurate linear registration and motion correction of brain images," *NeuroImage*, vol. 17, pp. 825–841, Oct. 2002.

[97] R. W. Cox and J. S. Hyde, "Software tools for analysis and visualization of fMRI data," *NMR in Biomedicine*, vol. 10, pp. 171–178, June 1997.

[98] J. D. Power, A. Mitra, T. O. Laumann, A. Z. Snyder, B. L. Schlaggar, and S. E. Petersen, "Methods to detect, characterize, and remove motion artifact in resting state fMRI," *NeuroImage*, vol. 84, pp. 320–341, Jan. 2014.

[99] Y. Behzadi, K. Restom, J. Liau, and T. T. Liu, "A component based noise correction method (CompCor) for BOLD and perfusion based fMRI," *NeuroImage*, vol. 37, pp. 90–101, Aug. 2007.

[100] D. Mascali, M. Moraschi, M. DiNuzzo, S. Tommasin, M. Fratini, T. Gili, R. G. Wise, S. Mangia, E. Macaluso, and F. Giove, "Evaluation of denoising strategies for task-based functional connectivity: Equalizing residual motion artifacts between rest and cognitively demanding tasks," *Human Brain Mapping*, vol. 42, pp. 1805–1828, Feb. 2021.

[101] P. Pinel and S. Dehaene, "Beyond hemispheric dominance: Brain regions underlying the joint lateralization of language and arithmetic to the left hemisphere," *Journal of Cognitive Neuroscience*, vol. 22, pp. 48–66, Jan. 2010.

[102] Z. Gao, W. Zhao, S. Liu, Z. Liu, C. Yang, and Y. Xu, "Facial emotion recognition in schizophrenia," *Frontiers in Psychiatry*, vol. 12, May 2021.

[103] M. G. Calvo and D. Beltrán, "Recognition advantage of happy faces: Tracing the neurocognitive processes," *Neuropsychologia*, vol. 51, pp. 2051–2061, Sept. 2013.

[104] M. G. Calvo and L. Nummenmaa, "Perceptual and affective mechanisms in facial expression recognition: An integrative review," *Cognition and Emotion*, vol. 30, pp. 1081–1106, July 2015.

[105] L. Nummenmaa and M. G. Calvo, "Dissociation between recognition and detection advantage for facial expressions: A meta-analysis.," *Emotion*, vol. 15, pp. 243–256, Apr. 2015.

[106] N. I. Muros, A. S. García, C. Forner, P. López-Arcas, G. Lahera, R. Rodriguez-Jimenez, K. N. Nieto, J. M. Latorre, A. Fernández-Caballero, and P. Fernández-Sotos, "Facial affect recognition by patients with schizophrenia using human avatars," *Journal of Clinical Medicine*, vol. 10, p. 1904, Apr. 2021.

[107] C. G. Kohler, T. H. Turner, R. E. Gur, and R. C. Gur, "Recognition of facial emotions in neuropsychiatric disorders," *CNS Spectrums*, vol. 9, pp. 267–274, Apr. 2004.

[108] F. H. Netter, *Atlas of human anatomy*. Elsevier, 2019.

[109] C. Ferrari, A. Ciricugno, C. Urgesi, and Z. Cattaneo, "Cerebellar contribution to emotional body language perception: a TMS study," *Social Cognitive and Affective Neuroscience*, vol. 17, pp. 81–90, Oct. 2019.

[110] N. S. van den Berg, R. B. Huitema, J. M. Spikman, G.-J. Luijckx, and E. H. F. de Haan, "Impairments in emotion recognition and risk-taking behavior after isolated, cerebellar stroke," *The Cerebellum*, vol. 19, pp. 419–425, Feb. 2020.

[111] N. Kuroki, M. E. Shenton, D. F. Salisbury, Y. Hirayasu, T. Onitsuka, H. Ersner, D. Yurgelun-Todd, R. Kikinis, F. A. Jolesz, and R. W. McCarley, "Middle and inferior temporal gyrus gray matter volume abnormalities in first-episode schizophrenia: An MRI study," *American Journal of Psychiatry*, vol. 163, pp. 2103–2110, Dec. 2006.

[112] V. M. Goghari, A. W. MacDonald, and S. R. Sponheim, "Temporal lobe structures and facial emotion recognition in schizophrenia patients and nonpsychotic relatives," *Schizophrenia Bulletin*, vol. 37, pp. 1281–1294, May 2010.

[113] G. Leng and M. Ludwig, "Intranasal oxytocin: Myths and delusions," *Biological Psychiatry*, vol. 79, pp. 243–250, Feb. 2016.

[114] M. Valstad, G. A. Alvares, M. Egknud, A. M. Matziorinis, O. A. Andreassen, L. T. Westlye, and D. S. Quintana, "The correlation between central and peripheral oxytocin concentrations: A systematic review and meta-analysis," *Neuroscience &amp Biobehavioral Reviews*, vol. 78, pp. 117–124, July 2017.

[115] S. Fan, Z. Shen, B. L. Koenig, T.-T. Ng, and M. S. Kankanhalli, "When and why static images are more effective than videos," *IEEE Transactions on Affective Computing*, vol. 14, pp. 308–320, Jan. 2023.

[116] E. R. Bradley and J. D. Woolley, "Oxytocin effects in schizophrenia: Reconciling mixed findings and moving forward," *Neuroscience &amp Biobehavioral Reviews*, vol. 80, pp. 36–56, Sept. 2017.

[117] R. N. Boubela, K. Kalcher, W. Huf, E.-M. Seidel, B. Derntl, L. Pezawas, C. Našel, and E. Moser, "fMRI measurements of amygdala activation are confounded by stimulus correlated signal fluctuation in nearby veins draining distant brain regions," *Scientific Reports*, vol. 5, May 2015.

[118] S. B. Manuck, S. M. Brown, E. E. Forbes, and A. R. Hariri, "Temporal stability of individual differences in amygdala reactivity," *American Journal of Psychiatry*, vol. 164, pp. 1613–1614, Oct. 2007.

[119] I. Lipp, K. Murphy, R. Wise, and X. Caseras, "Understanding the contribution of neural and physiological signal variation to the low repeatability of emotion-induced BOLD responses," *NeuroImage*, vol. 86, pp. 335–342, Feb. 2014.

[120] K. Phan, T. Wager, S. F. Taylor, and I. Liberzon, "Functional neuroanatomy of emotion: A meta-analysis of emotion activation studies in PET and fMRI," *NeuroImage*, vol. 16, pp. 331–348, June 2002.